Relating shale mineralogy and microstructure to swelling activity: using Na-bentonite/sand pellets as a synthetic shale

TARA LEELA GRACE KAUR LOVE

Relating shale mineralogy and microstructure to swelling activity: using Na-bentonite/sand pellets as a synthetic shale

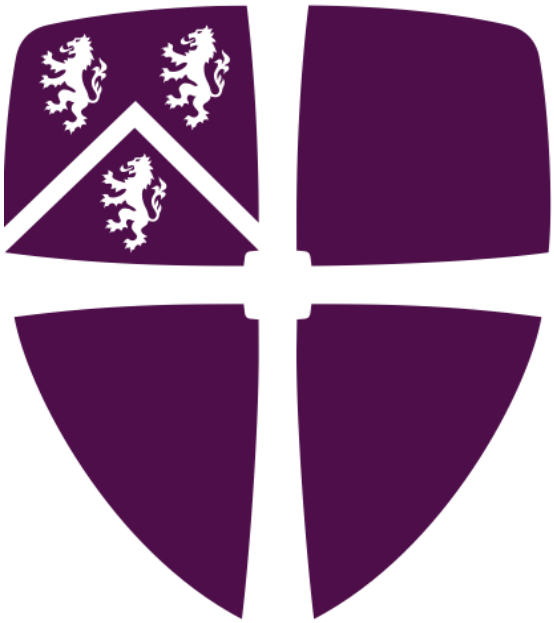

Tara Leela Grace Kaur Love

Department of Earth Sciences, Durham University

MSc by Research Thesis

Hatfield College **October 2019**

I hereby declare that all information in this document has been obtained and presented in accordance with academic rules and ethical conduct. I also declare that I have fully cited and referenced all material, and results, that are not original to this work

Tara Love

ABSTRACT

Shale formation instability presents significant challenges to oil and gas operations. Clay minerals within shale may react with water-based fluids (WBFs) causing swelling, aggregation of shale cuttings on the drill string (bit balling) and potentially wellbore collapse. Factors affecting clay hydration downhole still require investigation.

The swelling response of shale was studied to understand swelling-mechanisms, and potential causes, that lead to shale instability. The relationship between mineralogical composition, compaction pressure and formation age were investigated and related to shale-fluid interaction mechanisms within a wellbore region.

Expansive clay minerals typically associated with swelling-related shale instability are smectite or mixed-layer clays. Wyoming bentonite (montmorillonite-clay) has high absorption and swelling rates when hydrated, and for this reason, was used as an analogue for rich sub-sea shale formations. Artificial shale cores were made by varying quartz content (0-30%) and quartz size fractions (125-250 μm, >250-300 μm and >300 μm). Sample preparation conditions were varied with two compaction pressures (44.25 MPa, 88.50 MPa) and three compaction-time (5, 8 and 10 minutes) intervals.

Clay swelling experiments frequently involve monitoring the one-dimensional displacement with time of an initially dry clay core as it imbibes water from a supply at its base. While KCl is predominantly used in drilling and completion fluids to reduce the hydration of shales and thereby swelling-related instability, the purpose of these novel experiments was to ascertain how mineralogy impacts swelling of shale. Therefore, NaCl brine (0.5 and 2 mol/L concentrations) was selected for the electrolyte to induce lattice expansion within the clay.

The data implies that increasing burial depth (i.e. pressure increase) has a less significant effect upon swelling and instability than previously thought. Instead, the age of the sediment (i.e. compaction time) appears to have the most significant impact upon the structure of the rock, and thereby, the swelling. Other variables that were found to have a significant effect on the maximum swelling of an artificial core were quartz (%) content and saline concentration (>0.5 mol/L).

Some formations with water-sensitive clays do not always exhibit swelling behaviour, and it can be challenging to predict the response of these rocks to aqueous fluids downhole. These results indicate that dispersing capabilities, cementation, bedding orientation (i.e. diagenetic history) and pore water chemistry are all significant variables when predicting or testing for shale stability.

ACKNOWLEDGEMENTS

I would like to first thank my supervisors, Professor Chris H. Greenwell and Dr Darren R. Gröcke; I would, and could, not have achieved many of my dreams without their continued support during my undergraduate career, this and other projects. Thanks also for their active encouragement and support in my personal life and my pursuit of a PhD; they have shown me what it is to be both an excellent academic and supervisor, and I'll forever be in their debt. I'd like to thank the generosity of the Earth Science Department and awarding me with The Stephen Mills Postgraduate Studentship; which allowed me to afford to continue researching.

I couldn't have achieved this dissertation, or indeed anything, without the continued support and love from my parents, Jasminder and David Love. They have seen me through the good, bad and ugly, and given me the opportunities I never thought possible. Thanks also to my Godmothers, Eva and Hazel. I would also like to give my heartfelt thanks to Coran Hoskin, who supported me at my worst and encouraged me to be better; inspired me with his work ethic and helped me with his incredible Python knowledge. Thank you to Luke Mingaye for always being there for me as a wonderful friend, tolerating my extended sentences and fondness for semicolons.

I was lucky enough to be in an outstanding research group, where I had the pleasure of calling my colleagues, "friends". To those people in the Greenwell Group, and a special thanks must go to Mrs Catriona Sellick, for whom I will always be grateful for the out-of-hours company, dinner and advice, that meant I could finish my research for this Masters.

Also, thanks must go to those in the Earth Science Department, Durham University, from academic to admin staff you have all made this experience possible. Coming to Durham has been one of the best decisions of my life; it has offered me opportunities, experiences, qualifications and friendships.

Table of Contents

Introduction

The increasing production of oil and natural gas has caused the most accessible reservoirs, which are typically a porous and permeable formation beneath a cap rock (impermeable rock that prevents upward migration of the gas or liquid), to have become depleted. Conventional methods have had to evolve to extract resources at greater depths and temperatures with improved technologies. However, unconventional methods have become necessary, and only recently become profitable, to access hydrocarbon reserves found in atypical reservoirs (low-permeability source rock) that require horizontal drilling, and usually the addition of hydraulic fracturing (fracking).

A wellbore (Figure 1a) is drilled through many intervals of rock to produce hydrocarbons. Multiple casing strings (an assembled length of steel pipe) are cemented into place to assist with the stability of the drilled wellbore assembly. Besides, many wellbore completion accessories are put in place to prevent various challenges from occurring. Two such challenges are backflow - where a fluid flows from one section to another- as a result of pressure differences; and blowouts – the uninhibited upwards flow of formation fluids (Caenn *et* al., 2011; Civan, 2015). As illustrated in Figure 1b, to enable the drilling of a borehole, a drill bit (which is attached to the end of a drill string) bores its way down through sediment and bedrock to create the wellbore.

Drilling fluid (colloquially named ‘mud’) is pumped down from ground level through the drill string and exits through nozzles in the drill bit. Initially, the principal roles of muds in rotary drilling were to remove rock cuttings and act as a lubricant. As the need for hydrocarbons has increased, the diversification of methods to extract resources have caused muds to have a wider variety of functions (Caenn et al., 2011; Cook et al., 2011; Civan, 2015):

- Transport solid drill cuttings to the surface for separating
- Reduce the temperature and clean the drill bit
- Reducing friction between the equipment and the borehole
- Sustain the wellbore stability before casing (i.e. the favourable pressure difference between the wellbore and the rock formation)
- Form a filter cake that naturally forms against the rock to create a relatively impermeable seal across rock pores and over fractures
- Prevent inflow of fluids from permeable formations that have been drilled

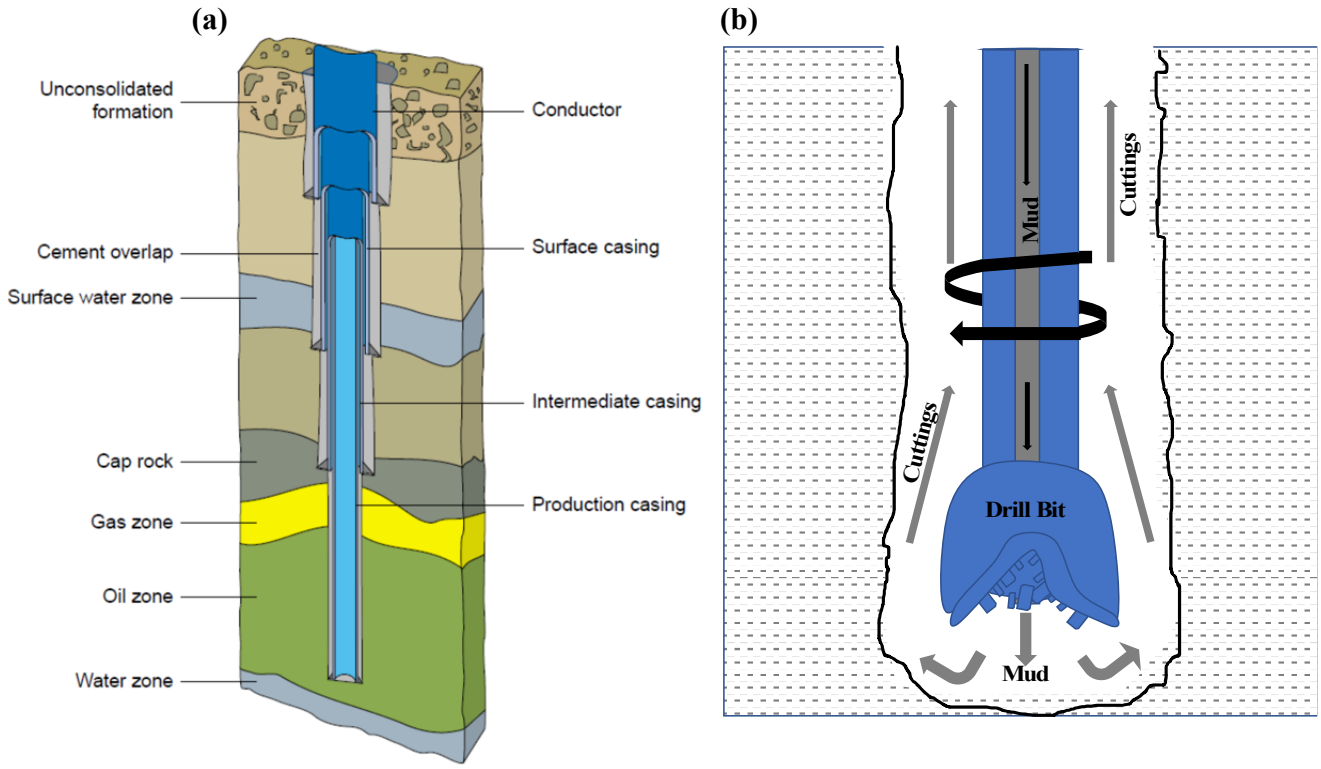

Figure 1*:* Illustrates **(a)** a conventional (typically vertical) wellbore and casing design which has been drilled through bedrock; it drills through a cap rock which has a reservoir formation (permeable rock containing oil and/or natural gas). Reproduced from IndustriMigas, 2014; and **(b)** a schematic of the lower wellbore: drilling fluid (mud) is pumped through the drill string and exits the drill bit through its head to lubricate/cool itself, and the return flow transports rock cuttings to the surface, where they are separated out.

Drilling fluids typically comprise of a continuous- (typically a liquid) and discontinuous (solids) phase. For the continuous phase, there is gas, aqueous fluids and non-aqueous systems, which are all used at different drilling stages and in formation-types. Whereas the solid phase (i.e. particles) is suspended in a base fluid to produce a mud, and this base fluid often defines their classification. The three main types of drilling fluids are water-base muds (WBMs), Oil-base muds (OBMs) and synthetic-base muds (SBM).

Water-base fluids typically have an aqueous (e.g. water or brines) base, whereas The OBMs and SBMs have an oil or synthetic base fluid as the continuous phase, and brine as the internal phase. The chemistry for these muds has become more complicated over time. The concept behind their uses has remained the same and muds continue to both maximise recovery and reduce the time taken to achieve first oil.

Although oil-base muds (OBMs) were widely used as they provided overall improved wellbore stability and are suitable across all the rock-types typically penetrated, environmental awareness has grown alongside the fossil fuel 'boom'. Pollution, widespread environmental damage, and climate change associated with both the production and use of hydrocarbons has resulted in more stringent restrictions of hazardous and toxic compositions used in these drilling fluids (Mody and Hale, 1993; Hale et al., 1993; Fink, 2015). As such, new aqueous-base drilling fluids have been developed to produce muds with equivalent capabilities shown by OBMs (Guo et al., 2011). The borehole in Figure 1(a) is an idealised representation of the formations. There would be many more interbedded rock intervals and many other potential complexities (e.g. faults and dipping bedding planes) in which the continuous phase (water) reacts (van Oort, 2003; van Oort et al., 2016; Gholami et al., 2018).

Wellbore instability is a significant challenge during the exploration for oil and natural gas (Cheatham, 1984; van Oort, 2003; Anderson et al., 2010; Caenn et al., 2011; Civan, 2011; Chan et al., 2019) and drilling through different types of rocks comes with new and specific challenges. Some of these challenges may be overcome by placing a casing shoe - a steel collar and cemented unit at the bottom of a casing string. When an open hole section becomes unstable, a casing shoe is used to confine the interval (i.e. ones with different characteristics, such as porosity and permeability requiring new drilling conditions), allowing the use of tailored muds. However, the quantity of these being placed are limited due to the complexity of the system (Caenn et al., 2011), such that the expense and time required outweighs their solution.

The inability to maintain a stable wellbore has been the primary cause for unprofitable drilling, and these instabilities account for close to 10-20 % of associated drilling costs (Albukhari et al., 2018); losing approximately $1-6 billion a year worldwide (Albukhari et al., 2018) across the oil and gas industry.

According to Caenn et al. (2011) and Cheatham (1984), wellbore instability relates to changes in borehole size relative to drilling equipment. These deviations from predicted size can vary to include dimensions of a borehole reduced due to soft plastic rock formations jamming themselves into the available space; hard and brittle rock breaking under applied stresses; and most commonly, shale instability.

Shale is a type of sedimentary rock found in marine basins (Gholami et al., 2018). It is a heterogeneous argillaceous (containing clay minerals) material with low permeability; exhibiting weakness parallel to the bedding plane i.e. fissility (Hawkes et

al., 2000; Nichols, 2009; Caenn et al., 2011; Wilson & Wilson, 2014). In the context of this research, ‘shale’ will relate to the oil industry definition: a fine-grained sedimentary rock primarily composed of silt and clay, broadly encompassing any mudrock (Nichols, 2009; Wilson & Wilson, 2014). This dominant clay-mineral composition has been identified as a significant cause of shale instability (O’Brien & Chenevert, 1973; Wilson & Wilson, 2014; van Oort et al., 2016) whereby there are two types of interaction: mechanical, which are independent of time and linked to the density of the drilling fluids, and Physico-chemical processes (Zeynali, 2012; Gholami et al., 2018), which are related to the shale-WBM interaction over time.

The interaction of aqueous drilling fluids with these clay minerals potentially induce clay swelling which can reduce wellbore strength resulting in ‘stuck pipe’, wellbore closure (causing ‘tight hole’), potential collapse and cave-ins; the hydration of drill cuttings enabling them to adhere to the drill bit assembly (‘bit balling’), which reduces penetration time; and finally, clay dispersion, resulting in the damage to the wellbore wall (van Oort, 2003; Anderson et al., 2010; Friedheim et al., 2011; Gholami et al., 2018; Chan et al., 2019).

Shales dominated by smectitic minerals are highly reactive with aqueous fluids, causing swelling. Clay swelling is a primary cause of shale instability. However, there are many non-smectitic formations (often illitic and mixed-layer clays) which experience dispersive-related (Wilson & Wilson, 2010) instability, instead of volume expansion.

Shale formations encompass close to ~75% of intervals penetrated during drilling through formations in a well. Problematic shales are the primary cause of wellbore instability and account for more than 90% (van Oort et al., 1996; Steiger & Leung, 1992; Wilson & Wilson, 2014; Gholami et al., 2018) of all instability.

In the last two decades, it has been reported that shale instability has been responsible for close to $500 million per annum (Anderson et al., 2010), and in the last seven years this has increased to an estimated $1 billion per year (Zeynali 2012) of costs associated to wellbore instability.

Aims

This study aims to investigate the swelling response of shales; to understand the swelling-mechanisms, and potential causes, that lead to shale instability. Laboratory experiments will make artificial cores to observe volume expansion experienced in reactive shales within a wellbore region.

This project will investigate how changing variables during the preparation of the samples, and while running swell-tests, changes the maximum vertical displacement and the rate of change for an experiment, and inferences will be made to relate artificial samples to real-shale.

Shale Instability and Clay Mineralogy

Shale Properties

The various types of shale instability experienced across wellbores indicate that not all shales are, or behave, the same. Problematic shales, or "reactive shales" (Anderson et al., 2010), have multiple properties which change with the depth of burial (i.e. compaction) and formation age (i.e. time) (Caenn et al., 2011; Wilson & Wilson, 2014), but they generally all contain a high clay mineral content (Anderson et al., 2010). The consensus for the leading cause for the unstable nature of shales is the interaction between these heterogeneous rocks and aqueous (where water is the base) fluids; these, in turn, are directly related to the quantity and type of clay minerals present in a specific formation, along with shales rock texture, structure and fabric (O'Brien & Chenevert, 1973; Wilson & Wilson, 2014). The clay minerals enable shale swell due to their hydrophilic and charged nature, allowing for cation exchange to (instability) occur (Wilson & Wilson, 2014). Figure 2 illustrates typical shale instability, typically associated with clay minerals. Clay minerals will be discussed in further detail to elucidate reasons behind their stability issues.

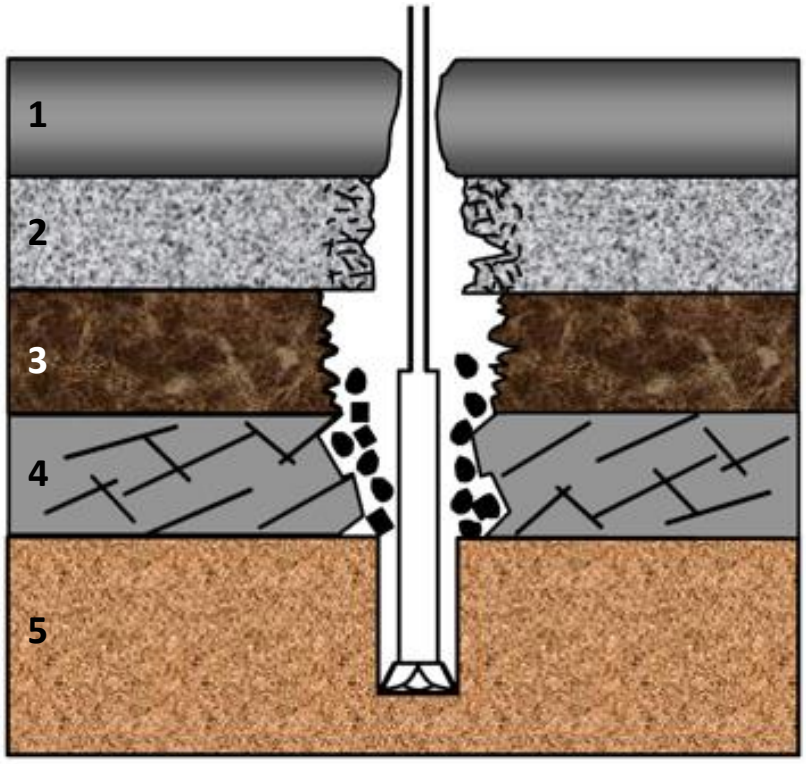

Figure 2: A schematic of shale instability experienced when drilling a wellbore, **(1)** is a soft, swelling shale; **(2)** brittle-plastic shale; **(3)** a brittle shale; **(4)** is a naturally fractured shale, and **(5)** is a competent rock formation. Adapted from Hawkes et al. (2000)

Properties of Clay Minerals

Clays are naturally occurring layered minerals, classified as phyllosilicates, with a mica-like, flaky structure; they have a crystalline nature, and the atomic structure of these crystals determines the properties. The clay minerals form from igneous rocks which have undergone weathering and decomposition (Grim, 1953; Anderson et al., 2010).

Clays are used across a wide array of industries, including pharmaceutical, oil and gas, chemical and waste disposal. They are used as liner materials for nuclear waste repositories and other waste containment, as an adsorbent (e.g. in water purification), used as a lubricant in drilling fluids and a variety of research. While clay minerals are the primary constituent of shales and mudrocks and often lead to their associated instability, they are also found in many other sedimentary formations. Sedimentary rocks that contain authigenic, pore-filling clays that have a sensitivity to water, will likely result in formation damage and permeability impairment.

Clay Minerals Structure

Crystal platelets stack together (face-to-face) to form a single clay flake. Individual crystal platelets are known as "unit layers", and their surfaces are referred to as "basal surfaces"; typically, clays consist of: an octahedral (O) sheet comprised of either aluminium (Al^{3+}), magnesium (Mg^{2+}) or iron (Fe^{3+}) oxides in octahedral coordination with oxygen atoms as shown in Figure 3; however, the sheet is called *dioctahedral* if the metal atoms are composed of aluminium, taking up two of the three sites. Similarly, the sheets are termed *trioctahedral* if the atoms are (and all three sites accounted for by) magnesium. In addition to a (typically octahedral) sheet of metal atoms, clays also consist of one or two silica oxide (Si^{4+}) tetrahedral (T) sheets, with each silicon atom being tetrahedrally coordinated with oxygen atoms (Grim, 1953; Anderson et al., 2010; Caenn et al., 2011). The bonding that occurs between the octahedral and tetrahedral sheets through sharing an oxygen atom is illustrated in Figure 4.

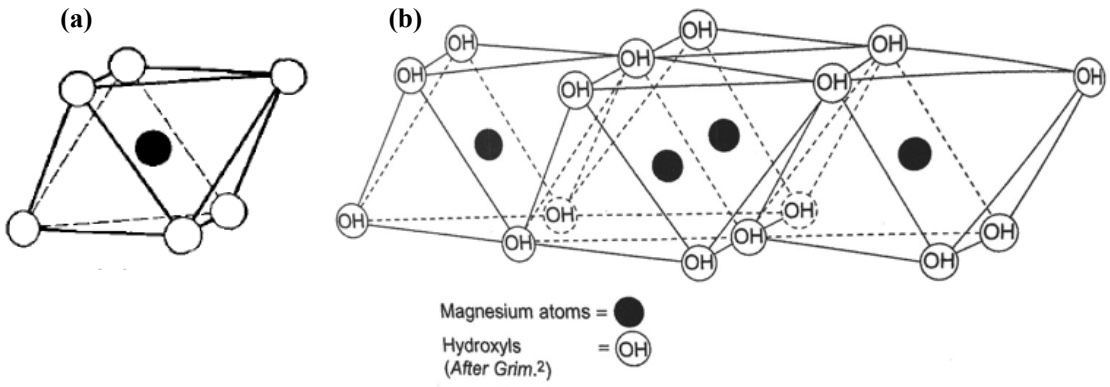

***Figure 3*:** Schematic description of clay structure components: **(b)** an octahedral unit. Sourced from Grim, 1953, and **(b)** an octahedral sheet structure of brucite. Sourced Caenn et al., 2011.

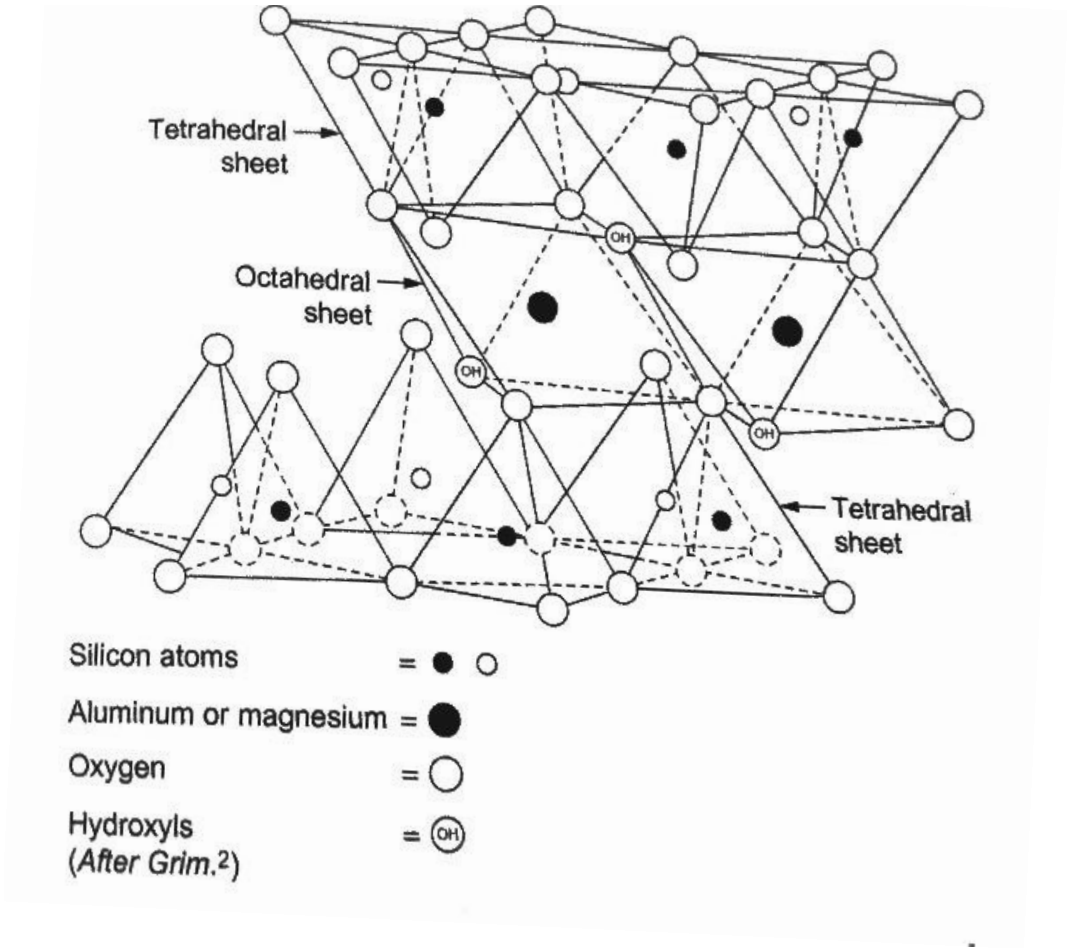

Figure 4: Bonding of a TOT (tetrahedral-octahedral-tetrahedral) with shared oxygen atoms. Sourced from Caenn et al. (2011) and Grim (1953).

When the sheets are tied together in the structure shown in Figure 6, the bonding between Oxygen and two T sheets here form something called the "Hoffman structure" (Hoffman et al., 1993; Caenn et al., 2014). Whereby, the T sheets share the oxygen atom at their apexes with the O sheet which has been inserted between the two (TOT structure), displacing two (of the three) hydroxyl atoms initially present, and exposing oxygen on both basal surfaces. Similarly, when only one T sheet is present, it is bonded in the same manner. Still, instead of having only oxygen networks exposed on both basal surfaces, one plane is instead a hydroxyl (OT structure). An example of a clay mineral in a TOT structure is montmorillonite, and an OT structure might be kaolinite.

The crystal lattice is formed by unit layers being stacked together face-to-face. The distance between a plane in one layer and the corresponding layer is coined as either: the c-spacing, the *001* or *basal spacing* (Figure 5). For a dehydrated TOT mineral (with a three-layer spacing) the basal spacing is approximately 9.2 Angstrom (Å = 10^{-7} mm), while it is 7.2 Å for an OT clay mineral for a two-layer spacing (Caenn et al., 2011). The adjacent sheets in a unit layer are held together by covalent bonds making them stable (Deer et al., 1992; Caenn et al., 2011); whereas, the crystal lattice layers are attracted together by van der Waals forces and secondary valencies between atoms next to each other (Caenn et al., 2011).

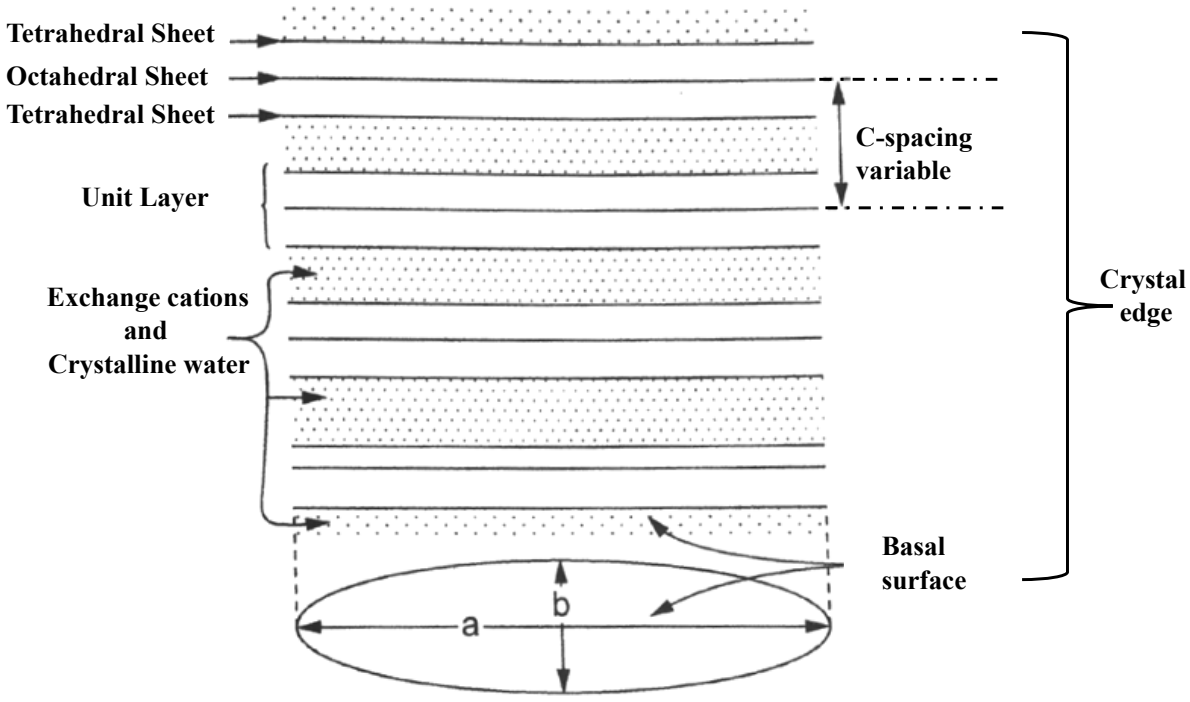

Figure 5: Schematic representation of an expanding three-layer, clay lattice. Sourced Caenn et al., 2011.

Clay minerals carry a charge arising from isomorphous substitutions of individual atoms in their structure for other atoms of a difference valence (Marshall, 1935; Caenn et al., 2011). If a metal atom such as aluminium (Al^{+3}) is replaced by a magnesium (Mg^{+2}) atom, then a negative potential at the crystals' surface would occur, which is compensated by the adsorption of a cation. The adsorbed cations can exchange with another species in the water and are coined the '*exchangeable cations'*; and substitutions happen when the sheets are either in an octahedral or tetrahedral arrangement.

Cations are absorbed onto the basal surface of the clay mineral. Cations, along with anions, are also held at the edges of the crystal because an interruption along with the c-axis results in broken valence bonds (Darley and Gray, 1988; Caenn et al., 2011). Both sets of ions may be exchanged with ions in an aqueous solution. The exchange reaction is controlled by the relative concentration of ions in each phase. The capacity at which cations are adsorbed called the cation exchange capacity (CEC).

Clay Swelling Mechanisms

Table 1 introduces the main types of clay and their structure, chemistry and associated instability problems. All the clay mineral-types listed adsorb water, but smectites (montmorillonite) assimilate more into their structure than the other classes, in part due to their expanding lattice. It is because of this that many academic and industrial experiments related to clay, or shale-swell use montmorillonite-enriched clays to encourage its volume to increase.

Two well-acknowledged swelling mechanisms:

1. Crystalline swelling (also referred to as 'surface hydration'): which results from adsorption of monomolecular layers of water onto the basal crystal surfaces on the external and internal (expanding lattice) layer. Exchangeable cations influence crystalline swelling because: (i) many of the cations are already hydrated, and (ii) the cations bond to the surface of the mineral - except for Na^{+} and Li^{+} which lightly bond and often diffuse away.
2. Osmotic swelling: Occurs when the concentration of cations between the layers is higher than the bulk aqueous solution (Caenn et al., 2011). Accordingly, the c-

spacing increases as water are drawn in between the layers and thereby allowing for the diffuse double layer (DDL).

Osmotic swelling usually results in a much more significant increase in vertical displacement (i.e. swelling) than that seen in crystalline swelling. However, the repulsive forces amidst the layers reduce in the osmotic, rather than the crystalline, region.

Diffuse Double Layer (DDL) Theory

The interlayer cations within a dry clay are held together by the negatively charged clay platelets. The negative charge in clay needs to be equilibrated by a surplus of cations. If these cations are present in an aqueous form, they will move through the solution to balance the ion concentration. However, this movement is prevented by the surfaces of the clay, which are negatively charged, and the stability between diffusive and electrostatic forces leads to an ion distribution next to the surface of the clay (Civan, 2007; Caenn et al., 2011). This prohibitive movement and associated change between forces are termed the ‘diffuse double layer’.

Table 1: Common clay minerals, their mineralogy and characteristic problems often found during drilling with aqueous solutions. Sourced from Grim (1953), O'Brien & Chenevert (1973), Deer et al. (2009), Caenn et al. (2010) and Wilson & Wilson (2014).

Clay Mineral	Chemical Elements	Morphology	Surface Area (m^2/gm)	Cation Exchange Capacity (meq/100g)	Characteristic Problems
Kaolinite	$Al_4[Si_4O_{10}](OH)_8$	Stacked plate or sheet	20	3-15	Loss of permeability due to mineral dispersing, migrating and potentially concentrating at pore throats. No lattice expansion.
Chlorite	$(Mg, Al, Fe)_{12}[(Si, Al)_8O_{20}(OH)_{16}$	Plates, fan, honeycomb	100	10-40	Essentially non-swelling due to a lack of interlayer water, unless a chlorite has been degraded (removing the brucite layer) allowing a degree of interlayer hydration and expansion. It may also precipitate gelatinous $Fe(OH)_3$, plugging pore throats.
Illite	$(K_{1–1.5}Al_4[Si_{7–6.5}Al_{1–1.5}O_{20}](OH)_{4)}$	Irregular with elongated spines or granules	100	10-40	These are interlayered: they are dispersive and are swelling clays (when leaching of potassium ions occur)
Smectite (montmorillonite)	$(1/2Ca, Na)_{0.7}(Al, Mg, Fe)_4$ $[(Si, Al)_8O_{20}]•nH_2O$	Irregular, wavy or wrinkled sheets	700	70-150	Highly expansive (i.e. swelling) and dispersible. Loss of microporosity, permeability and increased area.
Mixed-Layer	Illite-Montmorillonite Chlorite-Montmorillonite	Ribbons supported by filamentous structures	100-700	-	Dispersive, swelling (i.e. expansive), caving etc.

METHODOLOGY

Materials

The clay mineral used in this study was montmorillonite (as Na-bentonite), and this dry powder was combined with varying percentages (0, 10, 20 and 30%) of quartz with different grain sizes).

The Wyoming Na-bentonite GDM was purchased from the supplier Steetley Bentonite & Absorbents Ltd, Retford, U.K. The quartz (sand, pure, 40-100 mesh) was obtained from ACROS Organics.

The electrolyte used in this study was sodium chloride (NaCl), purchased from VWR International. Swelling tests were run using 200 mL deionised water (18.2 mol/LΩ.cm), 0.5 mol/L and 2 mol/L Sodium Chloride (NaCl) brine solutions. Where solutions were prepared using:

$$\text{Molarity } (M) = \text{moles of solute/ litres of solution} \quad \textbf{(1)}$$

Filter paper (Whatman, Grade 1, 25 mm circles) was used during swelling in the Swellometer.

Particle Sizing

The quartz was sieved using meshes to obtain size fractions: 125-250 μm, >250-300 μm and >300 μm. These sized fractions, along with a sample of dry, powdered Wyoming bentonite (PWB), were then analysed using a Morphologi® G3 particle characterisation system from Malvern® Instruments, to characterize quartz and bentonite particle size and shape to a resolution of 0.2 μm up to several millimetres. Analysis of dry powdered bentonite and quartz particles measured 1,000 – 10,000 individual particles.

In image analysis, the principal method to determine the size of a 3-dimensional particle is to convert the image to a 2-dimensional shape and measure its circle equivalent (CE) diameter, as illustrated in Figure 7.

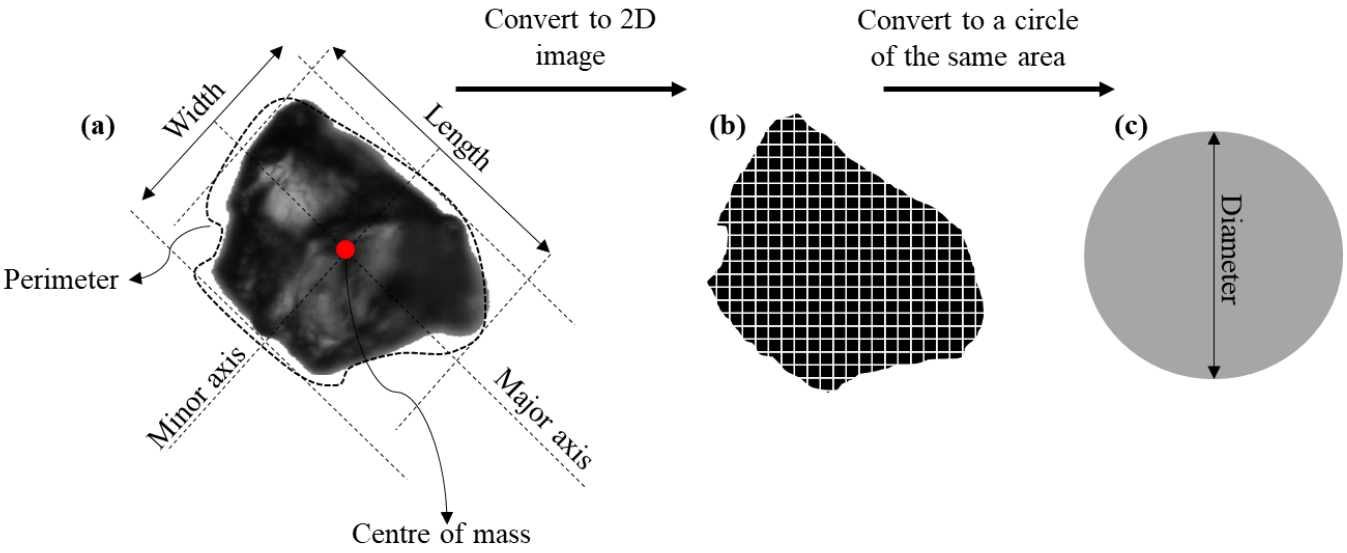

Figure 7: Schematic for the process used during image analysis: (a) is a 3D image of a quartz particle used in this study with measurement parameters, (b) 3D image is converted to a 2D shape with the same perimeter as the particle, and (c) the 2D image is converted into a circle with the same area, where the diameter is representative of the particle size.

Convexity is the convex perimeter (Fig.7a) of the particle exterior divided by a measured edge, and elongation is defined as 1 – Aspect Ratio (Width divided by length). Circularity (Figure 7) is the measure for the overall form of an object, and describes how close a particle is to a 'true' circle:

$$C = 2\sqrt{\frac{\pi A}{P}} \quad \textbf{(2)}$$

Where C is the circularity, *A* is the area, and P is the perimeter. This equation describes the circumference of the area of the two-dimensional particle, which has been converted to an equivalent area circle and is divided by the actual perimeter of that particle. This measure is sensitive to surface roughness and the total shape.

The most used metrics when using PSDs are D-Values: D10, D50 & D90, which are correspond to 10%, 50% and 90% of the cumulative mass.

Table 2: Particles used to produce artificial cores to run swelling experiments and their associated size and shapes measured using the Morphologi G3 particle characterization system. Values refer to D90 values.

Particle		Size			Shape		
		Length	Width	CE Diameter	Circularity	Convexity	Elongation
		(µm)					
Quartz	<125-250 µm	10.34	11.45	17.29	0.967	0.996	0.567
	250-300 µm	100.50	75.02	271.61	0.964	0.995	0.541
	> 300 µm	160.00	150.11	364.02	0.890	0.993	0.433
Clay	Wyoming Bentonite	16.32	6.66	8.27	0.806	0.996	0.515

An ideal circle has Circularity = 1, Convexity = 1 and Elongation = 0. Therefore, the powdered bentonite and quartz particles used in this study are:

1. Wyoming bentonite: Elongated, flat and ellipsoidal
2. Quartz: 125-250 μm and >250-300 μm are rounded to sub-rounded
3. whereas Quartz: >300 μm have grains that are relatively angular to sub-angular.

Preparation of 'synthetic shale.'

Synthetic Shale

The simplified 'synthetic shale' cores (pellets) were constructed using powdered Wyoming bentonite, with quartz at different concentrations and grain size; these were then compacted at a pressure representative of gas shales found in the North Sea oilfield.

The mixtures (see: *Table 3*) were weighed out, transferred into centrifuge tubes and mixed using a vortexer at 3,000 rpm for 5 minutes to homogenise the sample(s). Following this, the well-mixed powder was poured into the Specac evacuable pellet 20 mm die assembly, placed into the Specac manual hydraulic press, as seen in Figure 8 and (hand) pumped to either 44.25 or 88.50 MPa for the chosen time intervals: 5, 8, 10 and 30 minutes. The pressure was monitored and re-pumped to the desired value to ensure minimal variation (relaxation) during an interval.

Table 3 – Mixtures of Pure Wyoming Bentonite (PWB) and quartz used for the tests, with the solutions used for swelling experiments. For each pellet composition, the swelling tests were repeated with three grain sizes (250-125 μm, >250 300 μm and >300 μm), using three brine solutions (0 M, 0.5 M and 2 M NaCl), at 44.25 and 88.50 MPa at different times (5, 8, 10 and 30 minutes).

Artificial Core	Composition	
	Bentonite	Quartz
	(g)	
PWB	2.50	-
PWB:10	2.25	0.25
PWB:20	2.00	0.50
PWB:30	1.75	0.75

Synthetic shale cores were measured twice (centre and edge) using a digital calliper. The cores had an average (taken from approximately 800 cores) of 3.6 mm ± 0.15 mm thickness, 20 mm diameter and weighed 2.5 g ± 0.0025 g, with negligible variation to the mass, likely due to variation in humidity, or powder having become stuck to the inside of the die assembly. Once a core was made it was placed into a desiccator cabinet to reduce the effects of atmospheric moisture from hydrating the clay before running a swelling test; this would usually be kept inside for around 30 minutes between tests, and occasionally overnight for tests running the following morning.

Figure 8: Specac Hydraulic Press with manual hand-pump and pressure gauge.

Problems and developments during pellet preparation

Many samples 'stuck' to the polished steel pellets (gaskets), and the use of the desiccator cabinet prevented the worst of the effects. However, some samples required being cut out or dissolving to remove. Humidity and temperature had a noticeable impact on pellet preparation. Before sample compaction, the weighed powder was left to equilibrate to the air, and after that, sample preparation remained the same; and this alteration to methodology made slight improvements, albeit inconsistent.

Sticking issues, drawing parallels with 'bit-balling' in industry, were noticeably less for pure Wyoming Bentonite samples, when the steel pellets were freshly polished, reducing any defects on the surface. However, for mixed samples of bentonite and quartz, sticking and pellet collapse were real issues. For those samples pressed for 30 minutes, sticking caused the most significant problems, and not all planned tests were possible to run. Sticking issues were identified as being suction related, because if struck with force pellets would release from the gaskets with ease, except for 30-minute pellets which would not release, and had either broke in half or had to be dissolved in acetone.

Similarly, for samples with a quartz fraction of 30%, pellets were unable to maintain cohesion, especially for a grain size >300 μm. Unfortunately, the lack of cohesion meant that testing was unable to be finalised on all the 30% pellets; those results included in this project for the PWB:30 samples were solely for the smaller grain sizes, or not included due to an inability to ensure the pellets maintained their structure before swelling.

Problems related to a lack of cohesion could have potentially been countered by the addition of an adhesive, although this might have created a new problem, agglomeration (Luan et al., 2016). However, this was not implemented as this would have impacted the porosity and packing of the samples, thereby potentially interfering with swelling tests.

When introducing quartz to the system, when undergoing compaction, some pellets showed laminations and graded bedding (whereby there was a fining upwards sequence, with largest grains at the base of the pellet).

One hypothesis for this occurring was that the pressure and compaction caused the dry clay powder to liquefy and allow larger grains to pass through to the base. This effect was observed as both the content, and grain size of the quartz increased, with the most noticeable sand bands forming with compaction > 8 minutes.

A secondary cause could be that the mixing, whilst working for low sand content (< 20%) and smaller grain sizes, is not sufficiently long for the samples with greater quartz

volume; this mixing method could be altered in future experiments to extend the time or rotational speed until improvement is observed.

As demonstrated, pellet preparation and any differences between technician handling is critical and could explain issues with reproducibility in industry.

Swelling Measurements

To measure the one-dimensional (i.e. vertical) displacement for short-term, linear swelling of (compacted) synthetic shale pellets (bentonite/quartz mixtures), a novel instrument was used: 'the non-contact linear displacement meter' (Sellick et al., 2017; Mathais et al., 2017) which shall henceforth be referred to as either "Swellometer" or NC-LDM.

The Swellometer (Figure 9) uses four non-contact linear sensors to measure the distance between itself and a target. The sensor uses inductive technology, and the target influences the measurements. Therefore, before any tests, each sensor is calibrated using the Swellometer Software (Sellick et al., 2017), which incorporates an analytical solution from Mathias *et al*., 2017, into the software. This software aided with plotting swelling data from experiments. The Swellometer Software was set-up in accordance with the desired time, the number of measurements to be taken per minute (high resolution of 90 readings per minute) and with the correct associated calibration before beginning a test.

For a single test, four identical synthetic shale pellets were made, and placed into holders (Fig.9c) within the Swellometer on top of filter paper, sunk into its water bath shelf. The appropriate metal target disk for a specific sensor (Fig.9c) was placed onto the pellet, and then the sensor was screwed securely into place.

200 mL of deionised water or saline solution were poured into the bath through a hole in the centre where pellets were partially immersed; and so, the test started for the allocated time (short-term tests were run for 30 minutes) and four sets of data were produced (repeats). Individual tests were repeated if there were any inconsistencies to ensure that a minimum of four tests (i.e. data points) were taken and reproducible.

It should be noted that tests were performed at atmospheric pressure and room temperature; no confining pressure(s) were applied to the experimental system. However, future tests would be able to adapt the Swellometer, as it can perform non-linear swelling tests under pressure.

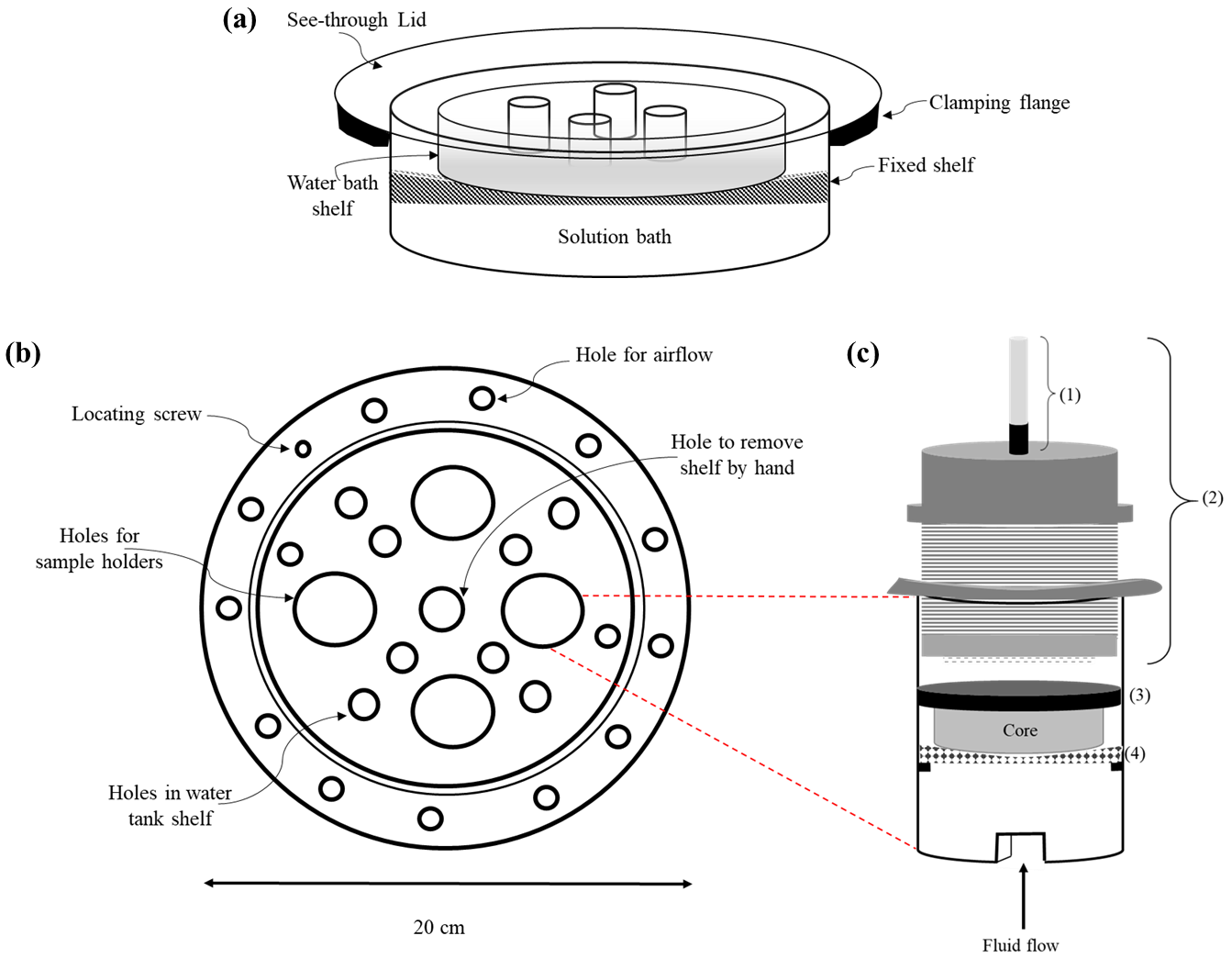

Figure 9 – Schematic of (a) The Non-Contact Linear Displacement Meter (NC-LDM), or 'Swellometer', (b) See-through plastic lid, (c) sample holder with (1) sensor wires connecting to computer with Swellometer Software, (2) Steel non-contact linear displacement sensor with thread, two nuts and sensor at the base, (3) Steel-target 1 mm steel disk placed on top of a pressed core, and (4) perforated metal sample support disk.

Data Analysis

Data produced were from 810 individual tests, producing approximately 200 data points. Analysis predominately comprised of interpreting vertical displacement (%) vs time (minutes) plots produced using Excel and Python 3.7.

Linear Regression

The following statistical method was used after processing data produced in swelling tests. Machine learning algorithms try to resolve two (main) challenges; to predict the continuous value of a specific data point (regression), and the class of a data point (classification). Linear Regression (LR) is a regression algorithm that uses a linear approach to simplify data. This technique identifies a linear relationship between two variables: X-axis is the independent variable and y-axis is the dependent variable (Figure 10). LR is a best-fit estimate for the plotted data. This method can be extended for numerous variables by using a multiple linear regression model, as outlined by Montgomery *et al*. (2012). This analysis was performed using: StatsModel version 0.10.1 (Seabold and Perktold, 2010).

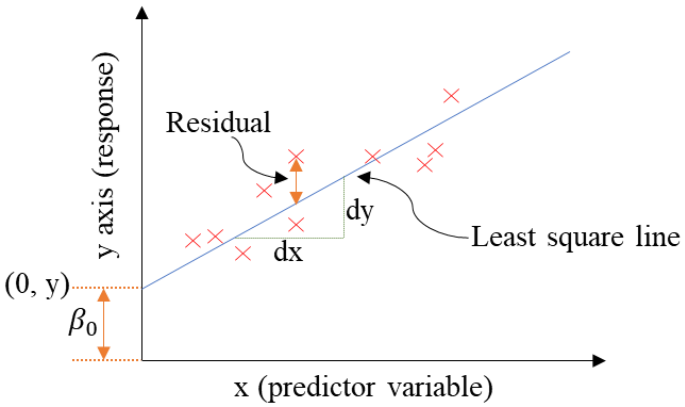

x = data point

$\beta_1 = \frac{dy}{dx}$

$Y = \beta_0 + \beta_1 x_1 + \beta_2 x_2 + \cdots + \beta_p x_p + \varepsilon$

Y is the response, dependent variable
β_0 is the coefficient
x_2 is the predictor, independent variable
ε is the random error (noise)

Figure 10 – Schematic of a simple two-variable x-y plot with Linear Regression applied to have the best-fit line for the plotted data. The equation is that for Multiple Linear Regression.

Analysis of Variance (ANOVA)

Analysis of the average maximum displacement across each variable (under combined pressures of 44.25 and 88.50 MPa) used the statistical method of Analysis of Variance (ANOVA) to separate the experimental variance of the data into different components to increase the precision of this statistical test i.e. hypothesis testing (Stahle and Wold., 1989). This can be used for multiple data groups (>2 groups) to understand the effect between the

variables (independent-dependent) better. To perform this analysis, the Python software SciPy, version 1.3.1 (Jones et al. (2001)), was used.

$$F = MST/MSE \quad \textbf{(3)}$$

Where F=ANOVA coefficient, MST=Mean sum of squares due to treatment, MSE=Mean sum of squares due to error.

Errors and Assumptions

While processing data exclusion criteria for tests (for each sensor repeat) were applied: if the range of vertical displacement from origin to the last point produced < 20% total difference, then this test would be excluded. The excluded values amounted to only 3.6% of individual tests, but the analysed data never used <3 sensor readings per experiment. Similarly, for the purposes of presenting data, the average displacement data were taken across all sensors (those meeting the inclusion criteria) per minute of the experiment; this enabled a shaded error region, rather than discrete bars, to be plotted on all lines.

For statistical significance, a threshold of p-value < 0.05 was selected based upon current standard practice and represented a reasonable balance between type I (false positive) and type II (false negative) errors. The p-value is the likelihood that based on the observed data, the null hypothesis is correct, 5% is low enough to reject the null hypothesis (i.e. no effect) and accept the alternative hypothesis (that there is an effect).

The necessary assumptions to proceed with an ANOVA analysis were considered: (1) The assumption of ‘independence of observations’ was believed to hold given the nature of the experimental design (e.g. calibration, resetting equipment, cleaning); (2) that the distribution of the residuals of the data were distributed normally because the data measured real-world phenomena, which invariably follows a normal distribution, and (3) the equality of group variance was not expected to deviate sufficiently to preclude the ANOVA analysis.

Results

This chapter will outline the results from short-term vertical displacement data of synthetic shales collected using The Non-Contact Linear Displacement Meter (NC-LDM).

Artificial cores comprised of Pure Wyoming Bentonite (PWB) with quartz for the following content: 0% (Bentonite-only), 10%, 20% and 30% quartz. Where quartz was introduced into the 'shale' preparation, size fractions were varied: 125-250 μm, >250-300 μm and >300 μm. These cores were prepared under different conditions by varying: The pressure at 44.25 and 88.50 MPa and time (5, 8 and 10 minutes) that they were compacted. Cores were partially submerged in either deionised water (labelled as 0 M) or an aqueous solution (sodium chloride at either 0.5 or 2 mol/L).

This chapter will be split into two sections: Bentonite-only and heterogeneous (PWB: Quartz) cores. Within these two sections, the effect that salinity/concentration, pressure, and compaction time will be outlined; and for mixed core (PWB: Quartz) a further description of how the percentage and grain size relate to vertical displacement of a sample.

Vertical Displacement of Bentonite Cores

Figure 11 illustrates a short-term swelling (30 minute) test for Pure Wyoming Bentonite cores that were pressed for 5, 8 and 10 minutes under a compaction pressure of either 44.24 or 88.50 MPa, and partially submerged in deionised water (0 M) or an aqueous saline solution: NaCl with a concentration of either 0.5 or 2 mol/L.

Compaction Pressure: 44.25 MPa

Deionised Water

PWB cores swollen in deionised water (Figure 11, top left) produced smooth curves for those samples prepared at 44.25 MPa for 5, 8 or 10 minutes:

- 5 minutes show a shallow, but steadily increasing trend (with only ~3% error), which gradually starts to plateau, reaching a peak of ~75%, with an initial gradient at an angle of ~45 degrees

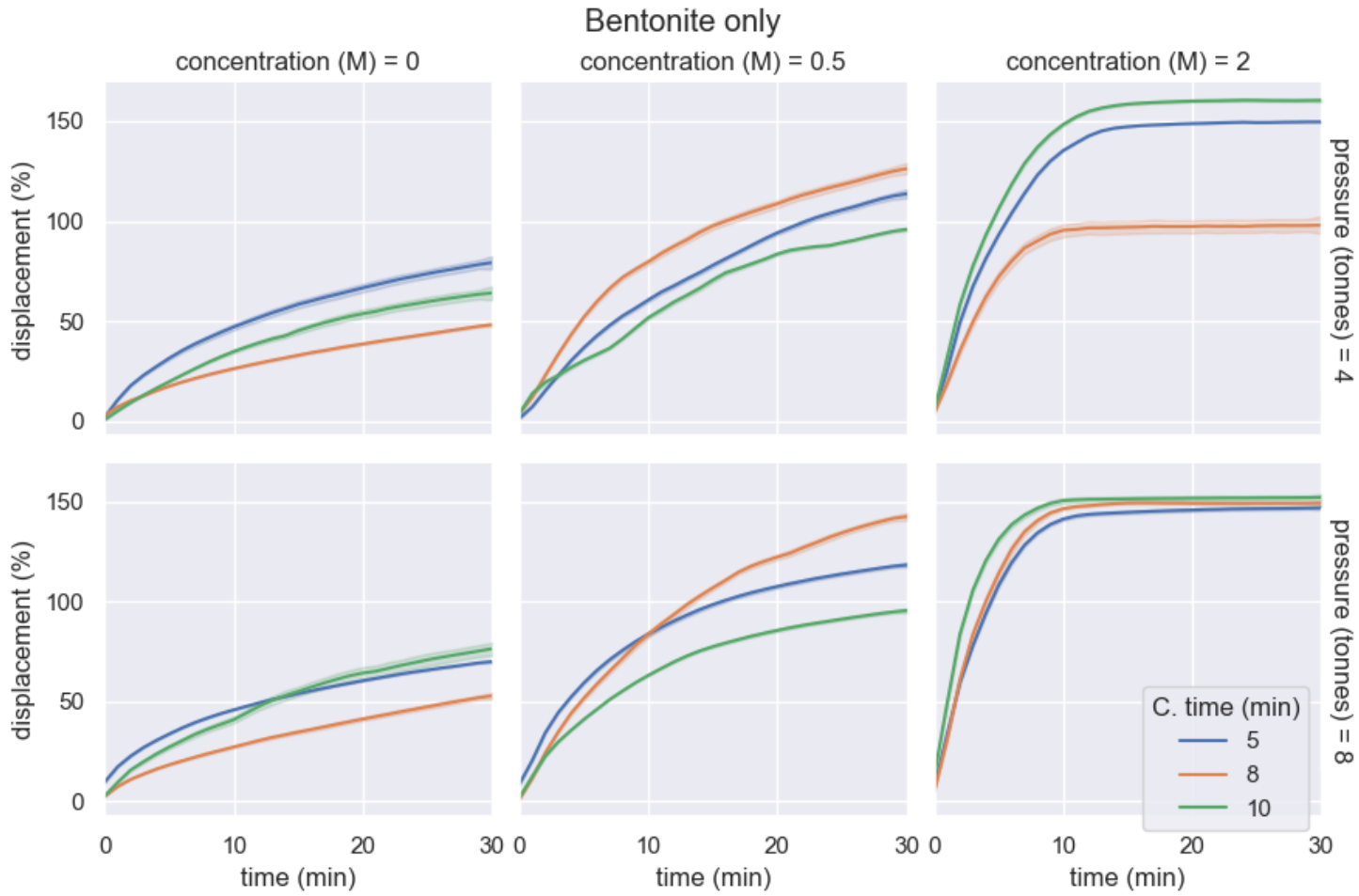

Figure 11: Bentonite-only displacement data across (the average of) all sensors per minute with a shaded error region (95% confidence interval of the mean). The plot identifies the concentration of the swelling solution: where 0 M = water, and sodium chloride has a concentration of either 0.5 or 2 mol/L; the pressure that the cores were prepared under (either 44.25 (4 tonnes) or 88.50 MPa (8 tonnes)). Each line represents the average vertical displacement for a test where pellets were compacted for either 5 (blue), 8 (orange) or 10 (green) minutes.

- 8 minutes shows a curve (with <1% error) that slightly increases, initially rising above the 10-minute line, then almost plateauing into a very gradual trend with a peak swell at 50%
- Moreover, the 10 minutes produced a curve (with ~3% error) almost parallel to the 5-minute line, but with a maximum swell at 30 minutes of ~65%. Initially, when compared to the blue curve, the displacement has a slightly shallower gradient, before imitating the trend and increasing above the 8-minute line within the first 5 minutes of the test. A small fluctuation, where displacement reduces by ~0.5% appears around 15 minutes.

Aqueous NaCl Solution: 0.5 mol/L

PWB cores swollen in 0.5 mol/L aqueous sodium chloride (NaCl) solution (Figure 11, top middle) produced slightly fluctuating, somewhat steeper curves for those samples prepared at 44.25 MPa for 5, 8 or 10 minutes:

- 5 minutes show an increasing trend (with < 3% error), reaching a peak of ~115%, with an initial gradient at an angle of ~45 degrees that steadily becomes steeper and intercepts the 10-minute line at around 4 minutes, whereby it has some slight perturbations (across the average), and gradually increases until slowly flattening out in parallel to the 8-minute line (but 10% less displacement). As illustrated in Figure 12b. Displacement increases the initial core (Fig.12a) by almost 280%.
- Eight minutes show a rapidly increasing trend (with < 3% error), reaching a peak of ~125%, with an initially steep incline until around 10 minutes into the test, where the curve starts to extend and level-off.
- Ten minutes produces a considerably fluctuating line (with ~1% error). In the first 2 minutes of the experiment, the curve rapidly increases with a similar gradient to the 8-minute plot; then it shows a change into a shallower linear trend until 8 minutes. After this point, displacement rapidly increases with a similar trend to the other two compression times. Finally, after 20 minutes with small fluctuations, the curve begins to flatten out and reach a peak of approximately 90%.

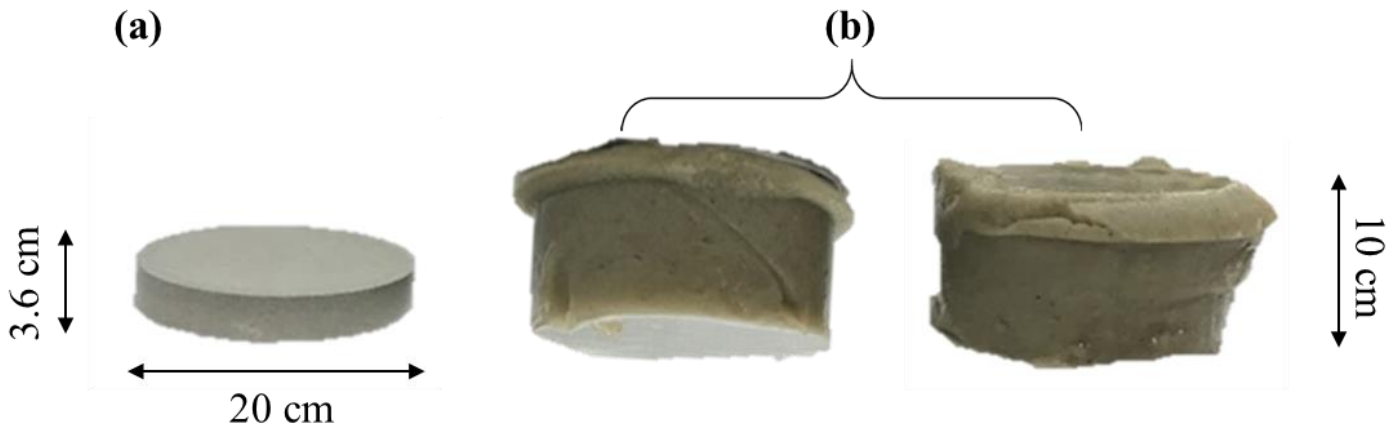

Figure 12: Photograph of bentonite compacted at 44.25 MPa for 5 minutes, swollen with 0.5 mol/L NaCl: **(a)** Original dry (bentonite) core and **(b)** how (a) appears after a short-term (30 minute) displacement.

Aqueous NaCl Solution: 2 mol/L

PWB cores swollen in 2 mol/L aqueous sodium chloride (NaCl) solution (Figure 11, top right) produced considerably steep curves, which plateau out and achieve their maximum swell in the first 10 minutes for all those samples prepared at 44.25 MPa for 5, 8 or 10 minutes:

- Five minutes shows a steep positive incline (with < 1% error), reaching a peak of ~150% by ~10 minutes, where there is a rapid change in the curve which completely flattens out.
- Eight minutes shows a slightly shallower (compared to the 5-minute line) rapid incline (with ~3% error). It initially has a rapid incline until around 10 minutes when it reaches a maximum of 100% into the test, after which it extends and levels-off
- Furthermore, the 10 minute produces a very steep rise (with ~1% error) early on, reaching its peak swell of 165% at 10 minutes into the test, quickly plateauing for the remainder of the test.

Compaction Pressure: 88.50 MPa

Deionised Water

PWB cores swollen in deionised water (Figure 11, bottom left) produced smooth curves, almost coincident to each, other for those samples prepared at 88.50 MPa for 5, 8 or 10 minutes:

- Five minutes show a shallow, but gradually increasing line (with only <1% error), which begins starts to flatten-off, reaching a peak of ~70%
- Eight minutes shows a considerably shallower (compared to the 5-minute line) curve (with <1% error). There is a very slight sharp incline that is parallel to the other two lines in the first two minutes; then the line swiftly becomes a linear trend, reaching a peak of 55%
- Furthermore, the 10 minute produces a curve (with ~3% error) parallel to the 5-minute plot until it reaches 10 minutes into the test; then it steadily increases and levels off to a peak at 75% with minor fluctuations in the trend.

Aqueous NaCl Solution: 0.5 mol/L

PWB cores swollen in 0.5 mol/L aqueous sodium chloride (NaCl) solution (Figure 11, top middle) produced slightly fluctuating, somewhat steeper curves for those samples prepared at 88.50 MPa for 5, 8 or 10 minutes:

- Five minutes shows a constant rate of change (error < 1%) with a maximum swell of 120%.
- Eight minutes shows a rapidly increasing linear trend until small fluctuations slow the rate of change, gradually reaching its peak displacement at 140%.
- And the 10 minute shows an initial rapid rate of change in the first 4 minutes, then the curve becomes more constant and gradually reaching a peak at 95%.

Aqueous NaCl Solution: 2 mol/L

PWB cores swollen in 2 mol/L aqueous sodium chloride (NaCl) solution (Figure 11, top right) produced considerably steep curves coincident with each other, which plateau out and achieve their maximum swell in the first 10 minutes for all those samples prepared at 88.50 MPa for 5, 8 or 10 minutes:

- Five-minutes shows a very steep, rapid change in rate (with < 1% error), reaching ~140% by ~10 minutes, where there is a rapid change in the curve which completely plateaus, and minimal swell occurs after that until it reaches 150%
- Eight minutes shows a rapid and steep incline (with <1% error). It initially has a rapid incline until around 10 minutes when it reaches 148%, after which it extends and levels-off increasing by only slightly to peak displacement of 150%
- And the 10 minute produces a very steep and rapid rate of change (with ~1% error) early on, reaching its peak swell of 150% at 10 minutes into the test, quickly plateauing for the remainder of the test.

Vertical Displacement of Mixed Bentonite and Quartz Cores

Figures in this section illustrate short-term swelling (30 minutes) tests for Pure Wyoming Bentonite mixed with 10%, 20% and 30% quartz with various size fractions: 125-250 μm, >250-300 μm and >300 μm. These cores were prepared by varying the pressure (44.25 and 88.50 MPa) and time (5, 8 and 10 minutes) that they were compacted. Cores were partially submerged in either deionised water (labelled as 0 M) or an aqueous saline solution (sodium chloride at either 0.5 or 2 mol/L).

Compaction Pressure: 44.25 MPa

Deionised Water

Figure 13 shows displacement plots for mixed PWB and Quartz (at varying %) cores with different particle sizes (μm) swollen in deionised water for samples prepared at 44.25 MPa for 5, 8 or 10 minutes. This subsection will discuss these plots with increasing quartz content and decreasing grain size. All curves have an error < 3% (shown by the shaded region in the plots).

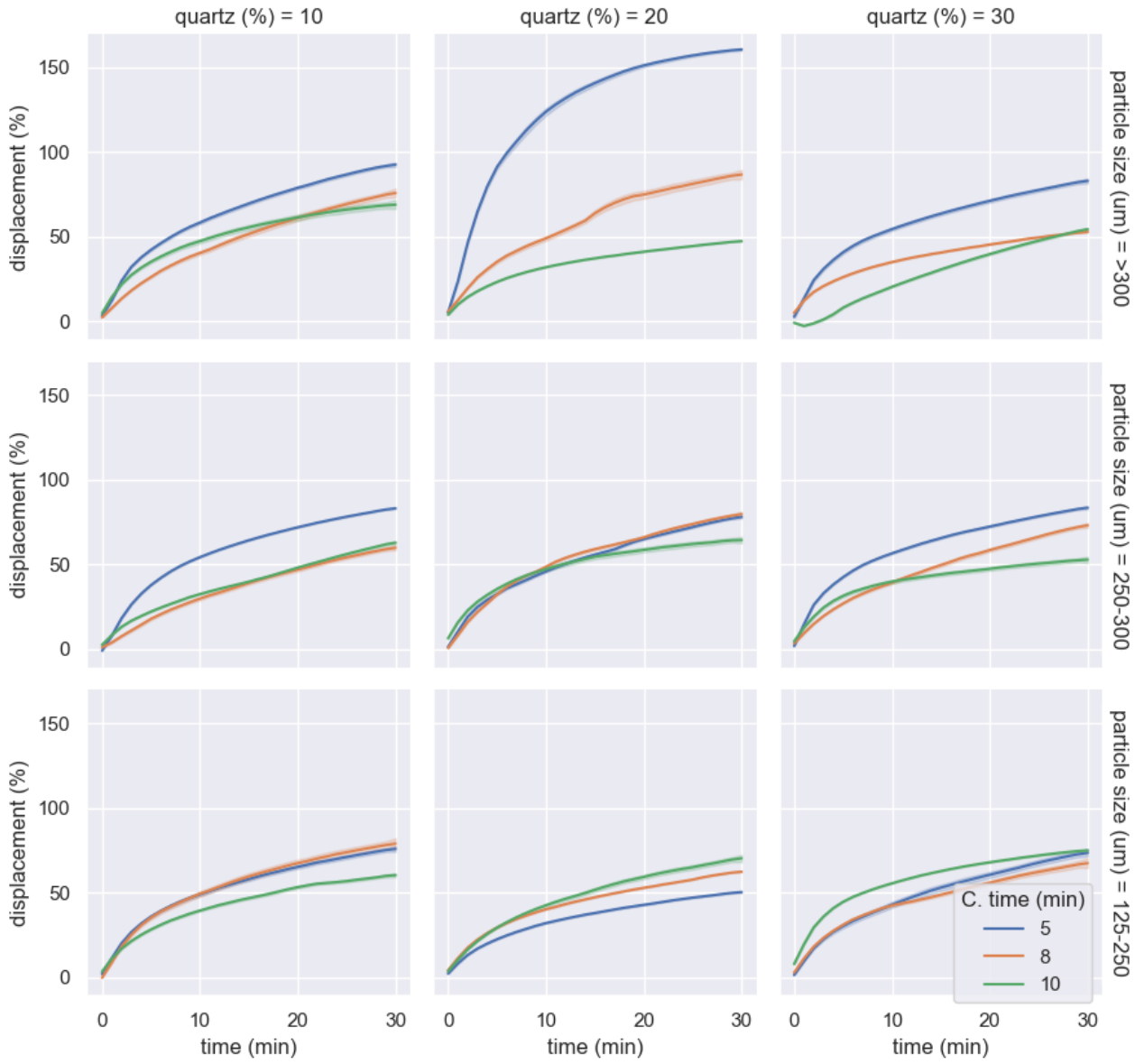

Figure 13: Mixed PWB and Quartz at 44.25 MPa in deionised water - displacement data across (the average of) all sensors per minute with a shaded error region (95% confidence interval of the mean). The plot identifies the quartz % of the cores and their particle size. Each line represents the average vertical displacement for a test where pellets were compacted for either 5 (blue), 8 (orange) or 10 (green) minutes.

10% Quartz

Particle size: >300 µm

Mixed PWB:10% quartz cores with a grain size >300 µm that were swollen in deionised water (Figure 13) produced a gradual increase in the rate of change, for those samples prepared at 44.25 MPa for 5, 8 or 10 minutes:

- Five minutes shows a somewhat rapid increase in the rate of change in the first 4 minutes, compared to the other plots, then gradually flattening out and reaching a peak swell of ~ 90%
- Eight minutes shows a steady, almost linear, rate of change until it lies parallel to 5 minutes and concludes the test with a maximum swell of ~ 75%
- Ten-minute samples initially have the same increase in displacement in the first 4 minutes as the 5-minute curve, until it changes direction slightly and deviates from the parallel five and 8-minute curves, almost plateauing. 10 minutes finished with a peak displacement value of ~70%

Particle size: 250-300 µm

Mixed PWB:10% quartz cores with a grain size 250-300 µm that were swollen in deionised water (Figure 13), produced a gradual, almost linear, increase in the rate of change, for those samples prepared at 44.25 MPa for 5, 8 or 10 minutes:

- 5 minutes shows a smooth curve that produces an increase in the rate of change until 10 minutes when it begins to extend to a peak of ~80%
- 8 minutes shows a steady, almost linear, rate of change until it lies coincident to the 10-minute data and concludes the test with a maximum swell of ~ 60%
- and the 10-minute samples initially has a somewhat steeper increase in displacement until 10 minutes, where it become almost linear and produces a plot very close to the 8-minute line, where it finishes slightly above with a peak at ~63%.

Particle size: 125-250 µm

Mixed PWB:10% quartz cores with a grain size 125-250 µm that were swollen in deionised water (Figure 13), produced a gradual increase in the rate of change with curves almost coincident to each other:

- 5 minutes shows a smooth curve that produces an increase in the rate of change until ~ 4 minutes when it begins to gradually rise and extend to a peak at ~71%
- 8 minutes shows a plot coincident to 5-minute until 15 minutes where it slightly diverges and sits slightly above with a maximum swell of ~75%
- 10-minute samples initially follow the same trend as the other two samples (5 and 8-minutes) until ~5 minutes when it diverges and sits parallel at about 10% lower, reaching a peak at ~60%.

20% Quartz

Particle size: >300 µm

Mixed PWB:20% quartz cores with a grain size >300 µm that were swollen in deionised water (Figure 13) produced a wide variation between curves for samples prepared at 44.25 MPa for 5, 8 or 10 minutes:

- 5 minutes produced a smooth curve that rapidly increases the rate of change from 0 – 150% in the first 10 minutes, after which it starts to increase to a peak of ~160% gradually
- 8 minutes shows a steady, almost linear, rate of change, until 15 minutes into the test when there is a positive fluctuation, and the data rapidly increases into a linear trend until it reaches a maximum displacement of 90%
- and the 10-minute samples shows a gradual and steady rate of change, reaching a peak displacement at 50%

Particle size: 250 - 300 µm

Mixed PWB:20% quartz cores with a grain size 250-300 µm that were swollen in deionised water (Figure 13) produced parallel, almost coincident, displacement curves for samples prepared at 44.25 MPa for 5, 8 or 10 minutes:

- The 5-minute plot shows a gradual increase in the rate of change in the first 5 minutes of the experiment, after which the curve lengthens into a linear trend reaching a peak displacement of ~80%
- The 8-minute line shows a curve like the 5-minute line, but with some fluctuations around 10 minutes into the test, when swelling increases above the 5-minute plot. It reaches a peak of ~80%
- 10 minute has a slightly more rapid increase in the rate of displacement until 8 minutes into the test, where the curve begins to shallow and flatten out with a maximum value at 60%

Particle size: 125 - 250 µm

Mixed PWB:20% quartz cores with grain size 125- 250 µm that were swollen in deionised water (Figure 13) produced similar, gradual, displacement curves for samples prepared at 44.25 MPa for 5, 8 or 10 minutes:

- 5 minutes has a shallow, gradual rate of change to a peak at ~ 50%
- 8 minutes have a smooth rate of change with a steeper slope to that of the 5-minutes curve, and after 10 minutes it starts to lengthen out to a peak of ~60%
- Furthermore, 10 minutes produces a curve coincident to the 8-minute line plot until 10 minutes, where it diverges to increase to a maximum displacement at 65% gradually.

30% Quartz

Particle size: >300 µm

Mixed PWB:30% quartz cores with a grain size >300 µm that were swollen in deionised water (Figure 13) produced some variation between curves for samples prepared at 44.25 MPa for 5, 8 or 10 minutes:

- 5 minutes have a steady increase in the rate of change and gradually starts to lengthen out after 8 minutes into the test, reaching a peak of ~ 80%
- 8 minutes produced a line that initially has the same rate of change as the 5-minute curve until 2 mol/Linutes into the test, where it starts to gradually flatten out around 20% less overall, with a peak value of ~50%

- and the 10-minute samples shows displacement did not begin until ~5 minutes into the test, after which the curve produced rapidly increased in the rate of change and then had a linear trend until it reached a maximum displacement value of ~50%

Particle size: 250 - 300 µm

Mixed PWB:30% quartz cores with a grain size 250-300 µm that were swollen in deionised water (Figure 13) similar, shallow, curves for samples prepared at 44.25 MPa for 5, 8 or 10 minutes:

- 5 minutes produced a smooth curve with a gradual rise in the rate of change, levelling off slowly to peak displacement of ~85%
- 8 minutes produced a curve with a slightly shallow gradient to the 5-minute plot with around 10% overall difference between the parallel lines, reaching a maximum value of 80%
- and the 10-minute data produced a curve which initially (when compared to its overall shape) gradually increases above the 8-minute line until 10 minutes into the test when it intercepts and plateaus to a maximum value of ~50%

Particle size: 125-250 µm

Mixed PWB:30% quartz cores with a grain size 125-250 µm that were swollen in deionised water (Figure 13) produced a wide variation between curves for samples prepared at 44.25 MPa for 5, 8 or 10 minutes:

- The 5-minute plots produced a line coincident with the 8-minute plot until 10 minutes, where they diverge slightly into a linear trend to a maximum displacement of ~75%
- 8 minutes shows a curve coincident to the 5-minute line until diverging, where it reaches a peak at ~70%
- Ten minutes produced a smooth curve, with an initially somewhat steep rate of change (when compared to this plot), gradually flattening out to a peak of ~75%. Although this has the same maximum swell, or close to, as the other two lines (5 and 8 minutes) the rate of change in the first 10 minutes of the test is much steeper and has a difference of ~20% between the curves.

Aqueous NaCl Solution: 0.5 mol/L

Figure 14 shows displacement plots for mixed PWB and Quartz (at varying %) cores with different particle sizes (μm) swollen in an aqueous 0.5 mol/L NaCl solution for samples prepared at 44.25 MPa for 5, 8 or 10 minutes. This subsection will discuss these plots with increasing quartz content and decreasing grain size.

10% Quartz

Particle size: >300 μm

Mixed PWB:10% quartz cores with a grain size >300 μm that were swollen in an aqueous 0.5 mol/L NaCl solution (Figure 14) produced a somewhat rapid increase in the rate of change, for those samples prepared at 44.25 MPa:

- 5 minutes shows a steep and rapidly increasing rate of change in the first 10 minutes of the test, after which it begins to lengthen out to a peak of ~170%
- 8 minutes shows a curve that begins with a relatively steep initial rate of change, parallel to the 10-minutes line, but at around 8 minutes into the experiment there appear to be some fluctuations where the rate of change increases somewhat more steeply to a maximum displacement of 140%
- The 10-minute curve produced is a smooth and gradual increase in the rate of change, with an initially steeper curve than the 8-minute line, until ~15 minutes when they intercept, and 10 minutes starts to flatten out to a peak value of 130%

Particle size: 250-300 μm

Mixed PWB:10% quartz cores with a grain size 250-300 μm that were swollen in an aqueous 0.5 mol/L NaCl solution (Figure 14) at 44.25 MPa produced:

- 5 minutes shows a smooth curve with a steep increase in the rate of change until 10 minutes into the test, where the line starts to lengthen out to a maximum peak of ~160%
- 8 minutes shows a more (relative to the 5-minute curve) gradual change in rate, with some small perturbations at around 8 minutes into the test, after which it becomes smooth and slowly extending to its final displacement value of 125%

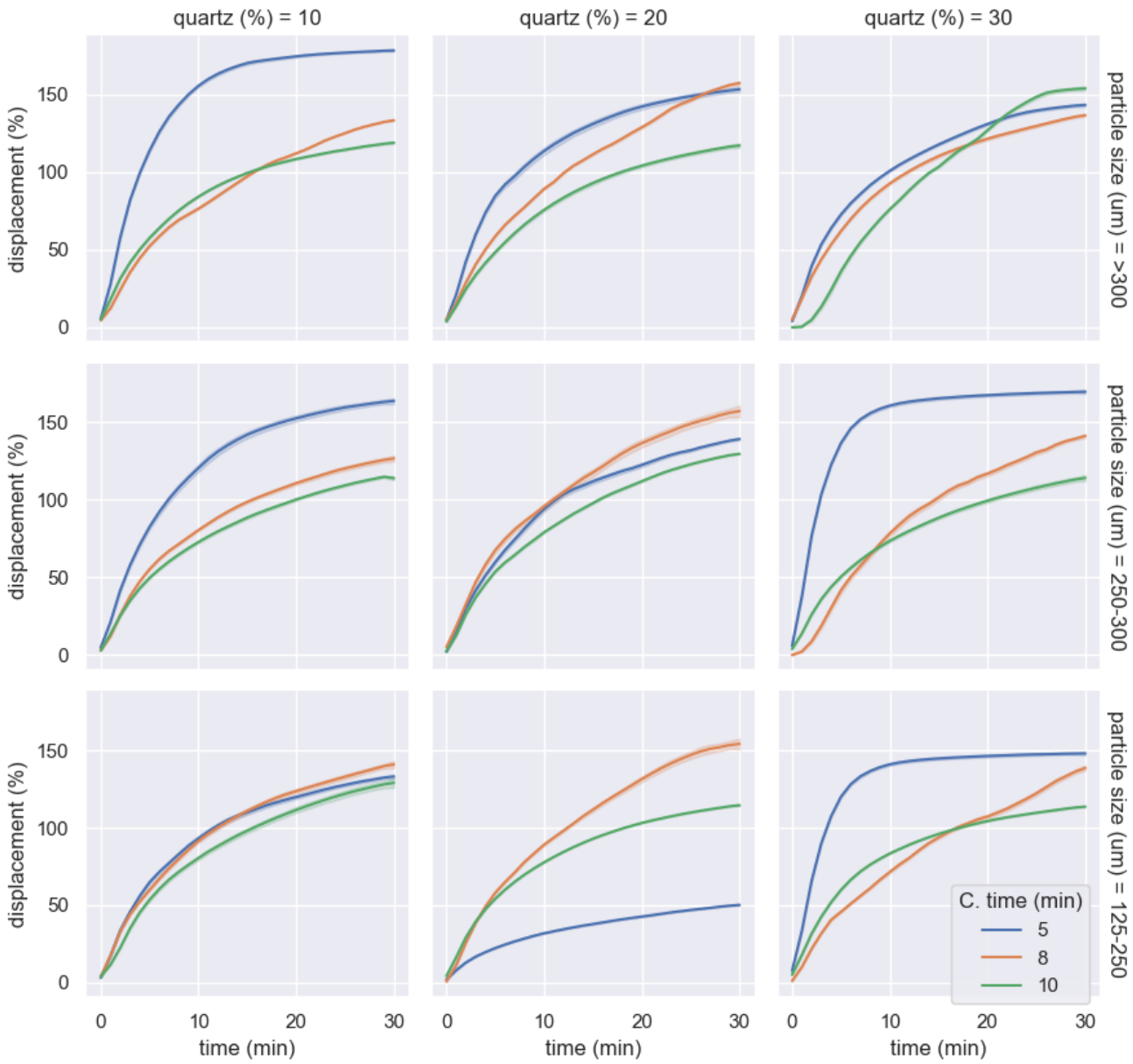

Figure 14: Mixed PWB and Quartz at 44.25 MPa in 0.5 mol/L NaCl solution - displacement data across (the average of) all sensors per minute with a shaded error region (95% confidence interval of the mean) – here all error is < 2%. The plot identifies the quartz % of the cores and their particle. Each line represents the average vertical displacement for a test where pellets were compacted for either 5 (blue), 8 (orange) or 10 (green) minutes.

- The 10-minute curve appears coincident with the 8-minute line until ~5 minutes into the test, when the curve begins to lengthen out until the final value (where there appears to be a slight drop in overall swell by ~2%) of ~115%.

Particle size: 125-250 μm

Mixed PWB:10% quartz cores with a grain size 125-250 μm that were swollen in an aqueous 0.5 mol/L NaCl solution (Figure 14), produced a gradual increase in the rate of change with curves laying close together:

- 5 minutes shows a smooth curve that produces an increase in the rate of change until ~ 10 minutes when it begins to gradually rise and extend to a peak at ~140%
- 8 minutes shows a plot almost coincident to 5-minute, with minor perturbations in the curve, until 15 minutes where it slightly diverges and increases slightly above to a maximum swell of ~145%
- The 10-minute samples initially follow a similar trend as the other two samples (5 and 8-minutes) until ~5 minutes when it diverges and sits parallel at about 10% lower, reaching a peak at ~135%.

20% Quartz

Particle size: >300 μm

Mixed PWB:20% quartz cores with a grain size >300 μm that were swollen in an aqueous 0.5 mol/L NaCl solution (Figure 14) produced some variation between curves for samples prepared at 44.25 MPa:

- 5 minutes produced a rapid increase in the rate of change, which starts to lengthen out to its maximum displacement value of ~150%
- 8 minutes shows a curve that has a steep, almost linear trend, increase for the first 5 minutes, after which it steadily increases with slight fluctuations from the trend, intercepting the 5-minute curve before its final swell value of 155%
- The 10-minute samples show a smooth and steady rate of change, reaching a peak displacement at ~125%.

Particle size: 250 - 300 µm

Mixed PWB:20% quartz cores with a grain size 250-300 µm that were swollen in an aqueous 0.5 mol/L NaCl solution (Figure 14) produced similar displacement curves for samples prepared at 44.25 MPa:

- 5 minute has a rapid increase (linear with slight perturbations) in the rate of change until ~10 minutes into the test, from which it starts to extend and lengthen out to 140%
- The 8-minute line shows a curve with a rapid rate of change that steadily increases to a maximum displacement value of 155% (this curve has <3% error, but the highest amount for Figure 14)
- Furthermore, the 10 minute has a slightly more rapid increase in the rate of displacement until 8 minutes into the test, where the curve begins to shallow and flatten out with a maximum value at ~125%.

Particle size: 125 - 250 µm

Mixed PWB:20% quartz cores with a grain size 125- 250 µm that were swollen in an aqueous 0.5 mol/L NaCl solution (Figure 14) produced varied displacement curves for samples prepared at 44.25 MPa:

- 5 minutes has a shallow, gradual rate of change to a peak at ~ 50%
- 8 minutes: Produces a rapid, and steep, rate of change which only starts to plateau in the last 5 minutes of the test to a maximum value of 150%
- 10 minutes: Shows a curve coincident to the 8-minute line plot until ~8 minutes into the test, where it diverges to lengthen out to peak displacement of ~120%

30% Quartz

Particle size: >300 µm

Mixed PWB:30% quartz cores with a grain size >300 µm that were swollen in an aqueous 0.5 mol/L NaCl solution (Figure 14) produced slight variation between curves for samples prepared at 44.25 MPa:

- 5 minutes produced a rapid increase in the rate of change, gradually flattening out from 20 minutes into the test to reach a maximum displacement value of ~145%

- 8 minutes produced a line parallel to the 5-minute plot, reaching a peak value of ~140%
- 10 minutes: Initially there appears to be delayed vertical displacement for the first 2 mol/Linutes of the test, after which there is a very steep (somewhat linear trend) until 25 minutes into the test where the curve begins to plateau to a maximum value at ~152%.

Particle size: 250 - 300 µm

Mixed PWB:30% quartz cores with a grain size 250-300 µm that were swollen in an aqueous 0.5 mol/L NaCl solution (Figure 14) similar, shallow, curves for samples prepared at 44.25 MPa:

- 5 minutes produced a very rapid increase in the rate of change in the first 8 minutes of the test, after which the curve lengthens out to a maximum displacement of ~170%
- 8 minutes shows a slight delay of displacement <2 mol/Linutes into the test, after which the rate of change rapidly increases, crossing the other two lines 20 minutes into the test and eventually plateauing around 5 minutes before the end of the experiment to a peak value of ~140%
- 10-minute produced a smoother curve which increases above the 8-minute line until ~8 minutes into the test when it intercepts and begins to gradually level out to a maximum value of ~115%

Particle size: 125-250 µm

Mixed PWB:30% quartz cores with a grain size 125-250 µm that were swollen in an aqueous 0.5 mol/L NaCl solution (Figure 14) produced a wide variation between curves for samples prepared at 44.25 MPa:

- 5 minutes produced a very rapid increase in the rate of change in the first 8 minutes of the test, after which the curve plateaus to a maximum displacement of ~150%
- 8 minutes shows a more slightly shallower rate of change, increasing rapidly from 5 minutes into the test (with slight perturbations), crossing the 10-minute curve 15 minutes into the test, and steadily to a peak value of ~145%

- 10-minute produced a smoother curve which increases above the 8-minute line until ~15 minutes into the test when it intercepts and begins to gradually level out to a maximum value of ~115%

Aqueous NaCl Solution: 2 mol/L

Figure 15 shows displacement plots for mixed PWB and Quartz (at varying %) cores with different particle sizes (μm) swollen in an aqueous 2 mol/L NaCl solution for samples prepared at 44.25 MPa for 5, 8 or 10 minutes. This subsection will discuss these plots with increasing quartz content and decreasing grain size.

10% Quartz

Particle size: >300 μm

Mixed PWB:10% quartz cores with a grain size >300 μm that were swollen in an aqueous 2 mol/L NaCl solution (Figure 15) produced a somewhat rapid increase in the rate of change of displacement, for those samples prepared at 44.25 MPa:

- 5 minutes shows a steep and rapidly increasing rate of change in the first 10 minutes of the test, after which it plateaus to a peak of ~140%
- 8 minutes shows a steep and rapidly increasing rate of change, parallel to the 5-minute plot, in the first 0 minutes of the experiment, after which it plateaus to a maximum displacement of ~145%
- The 10-minute curve produced a rapid increase in the rate of change in the first 5 minutes of the test, after which it smooths and gradually lengthens to a plateau, from ~15 minutes into the test, to a peak value of ~125%

Particle size: 250-300 μm

Mixed PWB:10% quartz cores with a grain size 250-300 μm that were swollen in an aqueous 2 mol/L NaCl solution (Figure 15) at 44.25 MPa produced:

- 5 minutes shows a sharp and rapid increase in the rate of change until it plateaus at ~170%, around 5 minutes into the test

- 8 minutes shows a rapid increase in the rate of change, with a slightly shallower gradient (relative to the 5-minute plot); however, this increases until it suddenly reaches a peak value of 170% after which it flattens out and appears to decrease its maximum displacement by ~5%
- The 10-minute curve to have a more gradual rate of change, which also plateaus 8 minutes into the test with a peak value of ~135%

Particle size: 125-250 μm

Mixed PWB:10% quartz cores with a grain size 125-250 μm that were swollen in an aqueous 2 mol/L NaCl solution (Figure 15), produced a steep increase in the rate of change with curves laying close together: All three curves (5, 8 and 10 minutes) initially have a steep linear trend coincident to each other, until 5 minutes into the test where they deviate from each other:

- 5 minutes gradually extends to flatten to a maximum displacement value of ~85%
- 8-minutes increases displacement (~5 % less than that of the 10-minute line) until it plateaus to 150% at 10 minutes into the test
- 10-minute samples initially follow a similar trend as the 8-minute curve, but it swells by ~5% more until 10 minutes into the test (with a peak value ~155%) when it seemingly plateaus and then gradually decreases by 5% at 20 minutes into the test.

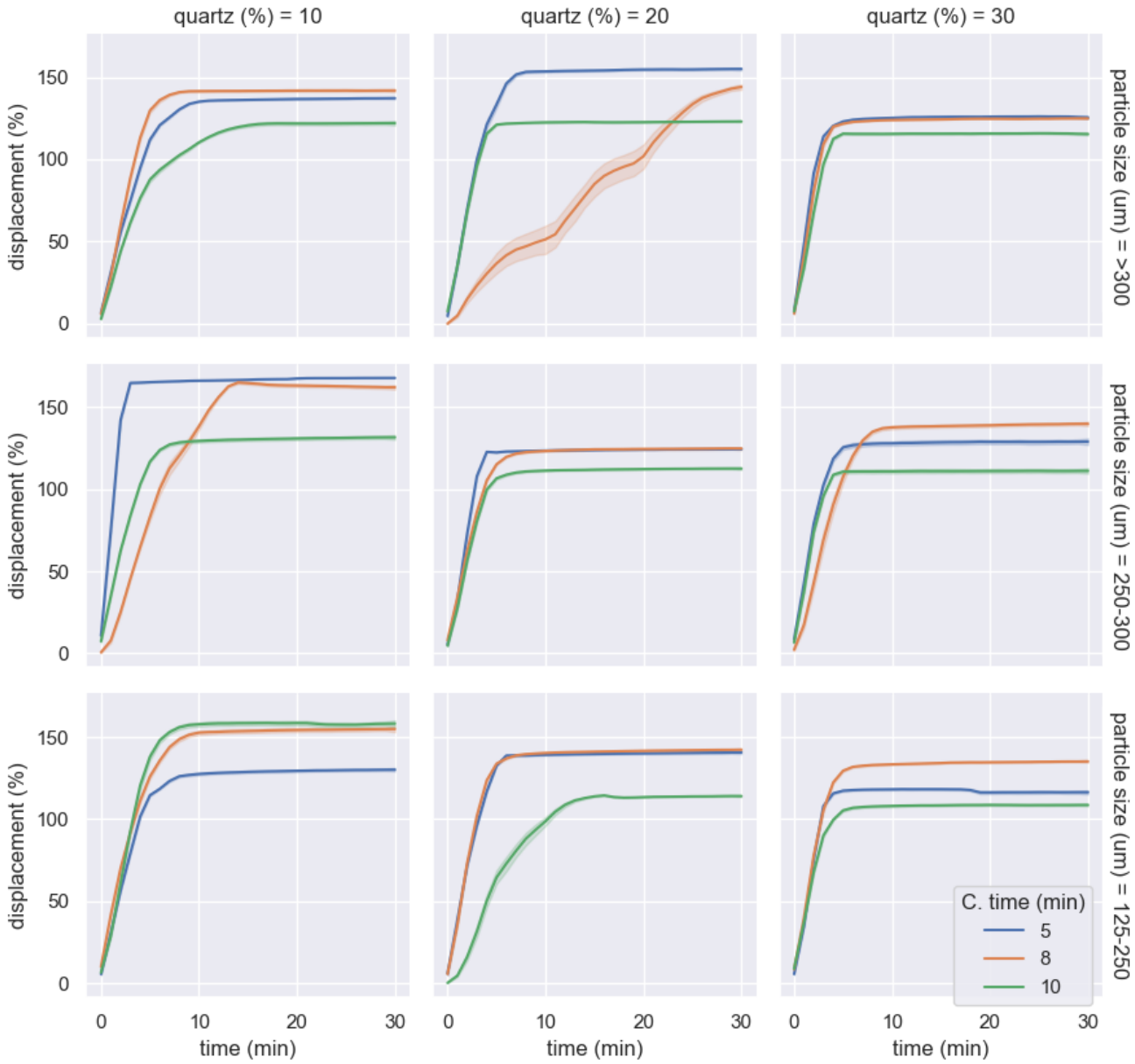

Figure 15: Mixed PWB and Quartz at 44.25 MPa in an aqueous 2 mol/L NaCl solution - displacement data across (the average of) all sensors per minute with a shaded error region (95% confidence interval of the mean) – here all error is < 2%. The plot identifies the quartz % of the cores and their particle. Each line represents the average vertical displacement for a test where pellets were compacted for either 5 (blue), 8 (orange) or 10 (green) minutes.

20% Quartz

Particle size: >300 µm

Mixed PWB:20% quartz cores with a grain size >300 µm that were swollen in an aqueous 2 mol/L NaCl solution (Figure 15) produced some variation between curves for samples prepared at 44.25 MPa:

- 5 minutes produced a rapid increase in the rate of change, which starts to lengthen out and eventually plateau to its maximum displacement value of ~150% by 8 minutes into the test
- Eight minutes shows a stepped-curve that steadily increases the rate of change; every 10 minutes the curve slightly flattens out and gradually increases before rapidly rising until the next step-change. It reaches a peak value of ~145%. The error decreases with time from ~20% to < 3% by the maximum swell.
- 10-minute line: Produces a steep, almost linear trend that is coincident with the 5-minute curve until they diverge at ~5 minutes into the, after which it plateaus to a maximum displacement of ~125%.

Particle size: 250 - 300 µm

Mixed PWB:20% quartz cores with a grain size 250-300 µm that were swollen in an aqueous 2 mol/L NaCl solution (Figure 15) produced similar displacement curves for samples prepared at 44.25 MPa: All three curves (5, 8 and 10 minutes) initially have a steep linear trend coincident to each other, until 5 minutes into the test where they deviate from each other and plateau out:

- 5 minutes initially has the highest swell of the plots at 5 minutes into the test and plateaus to have a maximum swell of ~125%
- The 8-minute line extends for another minute to reach a maximum swell of ~125% and have a plateau coincident with the 5-minute curve
- The 10-minute curve is slight shallower when it flattens out to a maximum value of 115%.

Particle size: 125 - 250 µm

Mixed PWB:20% quartz cores with grain size 125- 250 µm that were swollen in an aqueous 2 mol/L NaCl solution (Figure 15) produced some varied displacement curves for samples prepared at 44.25 MPa:

- The 5- and 8-minute plots produced curves that are coincident with each other: a very rapid increase in the rate of change in the first 5 minutes of the test, after which they plateau to achieve a maximum displacement of ~145%
- Ten minutes: Shows a curve with an initial swelling-delay <2 mol/Linutes into the test, which then rapidly increases the rate of change and gradually flattens out after 10 minutes of the test. A peak value of 120% is achieved at 15 minutes, then there is a slight decrease in displacement, and a plateau is reached.

30% Quartz

Particle size: >300 µm

Mixed PWB:30% quartz cores with a grain size >300 µm that were swollen in an aqueous 2 mol/L NaCl solution (Figure 15) produced almost identical displacement curves:

- The 5- and 8 minutes produced curves that are coincident with each other: a very rapid increase in the rate of change until a plateau is achieved with a maximum displacement of ~125% by t=5.
- The 10-minute curve is parallel to the other two curves, with a slightly shallower gradient. A plateau is achieved by 8 minutes of the test with a peak of ~115%.

Particle size: 250 - 300 µm

Mixed PWB:30% quartz cores with a grain size 250-300 µm that were swollen in an aqueous 2 mol/L NaCl solution (Figure 15) similar, somewhat steep, curves for samples prepared at 44.25 MPa:

- The 5-minute curves produced a rapid increase in the rate of change in the first ~4 minutes of the test, after which the curve lengthens out to a maximum displacement of ~130%

- 8 minutes produces a line that rapidly increases the rate of change (with a slightly shallower gradient that the two other time variables) and plateaus just before 10 minutes into the test, with a maximum displacement value of 145%
- 10-minute produced a rapid increase in the rate of change in the first ~4 minutes of the test, after which the curve lengthens out to a maximum displacement of ~120%

Particle size: 125-250 μm

Mixed PWB:30% quartz cores with a grain size 125-250 μm that were swollen in an aqueous 2 mol/L NaCl solution (Figure 15) produced a wide variation between curves for samples prepared at 44.25 MPa: All three curves (5, 8 and 10 minutes) initially have a steep linear trend coincident to each other until they diverge 5 minutes into the test, where they plateau out:

- 5-minutes curve achieve a maximum displacement of ~120% until there is a slight negative perturbation at 20 minutes of the test, and it decreases displacement by ~5%
- 8-minutes increases slightly before flattening out at 145%
- 10-minutes diverges and produces a peak value of 110%.

Compaction Pressure: 88.50 MPa

Deionised Water

Figure 16 shows displacement plots for mixed PWB and Quartz (at varying %) cores with different particle sizes (μm) swollen in deionised water for samples prepared at 88.50 MPa for 5, 8 or 10 minutes. This subsection will discuss these plots with increasing quartz content and decreasing grain size.

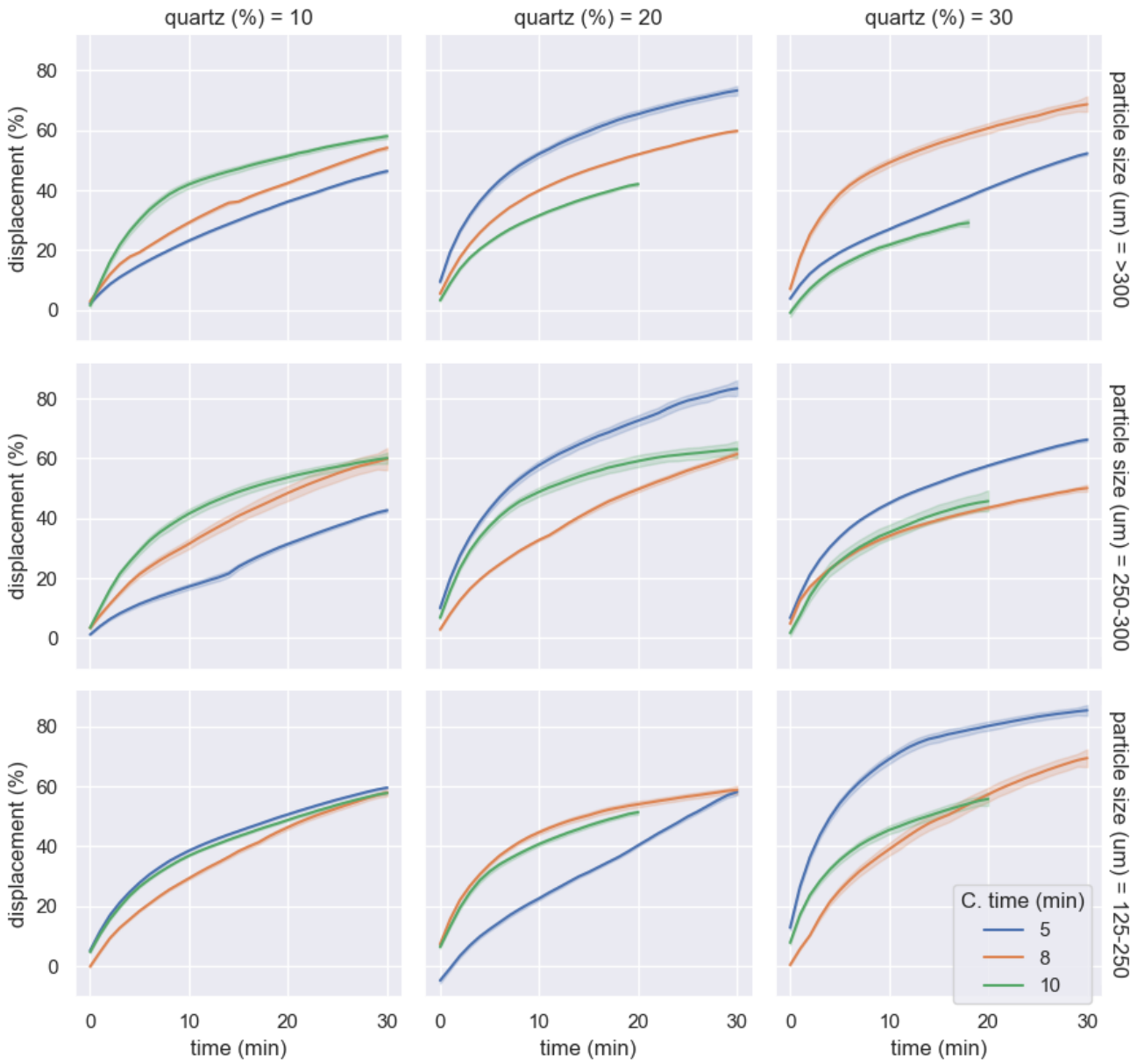

Figure 16: Mixed PWB and Quartz at 88.50 MPa in deionised water - displacement data across (the average of) all sensors per minute with a shaded error region (95% confidence interval of the mean) – here the average error <4%. The plot identifies the quartz % of the cores and their particle size. Each line represents the average vertical displacement for a test where pellets were compacted for either 5 (blue), 8 (orange), or 10 (green) minutes.

10% Quartz

Particle size: >300 µm

Mixed PWB:10% quartz cores with a grain size >300 µm that were swollen in deionised water (Figure 16) produced a gradual increase in the rate of change, for those samples prepared at 88.50 MPa:

- 5 minutes produce a line which slightly increases the rate of change into a steady linear trend with a peak of ~ 48%
- Eight minutes produces a curve with a steep rate of change in the first minute, which then fluctuates with two small step-changes. In between these small steps (one at 5 minutes which increases rate, and a second at 15 minutes which decreases displacement slightly), the line appears to have a linear trend until it reaches a peak at ~ 55%
- 10-minutes show a gradual increase in the rate of change; at 10 minutes, the curve starts to gradually extend and start to level-out until it reaches a peak at ~ 60%.

Particle size: 250-300 µm

Mixed PWB:10% quartz cores with a grain size 250-300 µm that were swollen in deionised water (Figure 16), produced a gradual, almost linear, increase in the rate of change, for those samples prepared at 88.50 MPa:

- 5 minutes shows a shallow linear trend until ~15 minutes into the test, where there is a rapid increase in displacement increasing to a peak at ~42%
- 8 minutes shows a gradual increase in the rate of change, until 10 minutes into the test where there is a more rapid increase in displacement producing a near-linear trend, reaching a peak of ~ 60%
- Furthermore, the 10-minute samples produce a line that gradually increases the rate of change to produce a smooth curve which gradually begins to level out and intercepts with the 8-minute curve at a maximum displacement of ~ 60%.

Particle size: 125-250 µm

Mixed PWB:10% quartz cores with a grain size 125-250 µm that were swollen in deionised water (Figure 16), produced a gradual increase in the rate of change with curves almost coincident to each other: 5 minutes and 10-minutes produce curves very close together; they have a gradual increase of the rate of swelling in the samples. Their slopes change at 10 minutes into the test to a slightly slower rate gradually levelling out to reach a peak of 60% and ~58%, respectively. Whereas the 8-minute curve shows an increasing rate of vertical displacement until it reaches a maximum value of ~ 57%.

20% Quartz

Particle size: >300 µm

Mixed PWB:20% quartz cores with a grain size >300 µm that were swollen in deionised water (Figure 16) produced almost parallel curves for samples prepared at 88.50 MPa: 5, 8 and 10 minutes all produce a smooth and steadily increasing rate of change which starts to shallow in its slope from t=10 until they reach their peak values of ~ 75%, 60% and 40% respectively.

Particle size: 250 - 300 µm

Mixed PWB:20% quartz cores with a grain size 250-300 µm that were swollen in deionised water (Figure 16) produced displacement curves for samples prepared at 88.50 MPa for the following time variables:

- The 5-minute plot shows a gradual increase in the rate of change in the first 10 minutes of the experiment, after which the curve lengthens with some small variations where it increases to a maximum displacement of ~ 85%
- 8 minutes gradually increase continually across the test to achieve a maximum value of ~60%
- The 10-minute line shows a curve similar to the 5-minute line, but when t=8 the curve changes slope to gradually level-off to a peak value of ~ 62%.

Particle size: 125 - 250 µm

Mixed PWB:20% quartz cores with a grain size 125- 250 µm that were swollen in deionised water (Figure 16) produced displacement curves for samples prepared at 88.50 MPa for the following time variables:

- 5 minutes increases the rate of change: The slope increases at 10 minutes and, again, at 20 minutes into the test until it reaches a peak of ~60%
- 8-minutes and 10 minutes produce a curve close to 10-minute line plot until ~ 8 minutes, where it diverges to gradually shallows its slope until it reaches ~ 60%.
- 10-minutes has a smooth rate of change with a steeper slope to that of the 5-minutes curve, and after 10 minutes it starts to lengthen out to a peak at ~ 50%

30% Quartz

Particle size: >300 µm

Mixed PWB:30% quartz cores with a grain size >300 µm that were swollen in deionised water (Figure 16) produced some variation between curves for samples prepared at 88.50 MPa for three-time variables:

- Five minutes gradually increased the rate of change, almost linearly from 10 minutes into the test. It attained a maximum displacement of ~50%
- 8-minutes produced a curve with a rapid increase in swelling rate until ~ 5 minutes into the test when the curve starts to gradually level-out to a peak of ~70%
- Moreover, 10 minutes which gradually increases the rate of change to a peak at ~30%.

Particle size: 250 - 300 µm

Mixed PWB:30% quartz cores with a grain size 250-300 µm that were swollen in deionised water (Figure 16) produced little variation between curves for samples prepared at 88.50 MPa for three-time variables: 5, 8 and 10-minute curves produce a gradual increase in the rate of change. Five minutes had the steepest gradient of the time-variables and started to elongate after 10 minutes with a peak at ~ 65%. Whereas, 8- and 10-minutes produced curves that lay close to each other, both levelling-out from 10 minutes and attaining a peak of ~50% and 45% respectively.

Particle size: 125-250 μm

Mixed PWB:30% quartz cores with a grain size 125-250 μm that were swollen in deionised water (Figure 16) produced some variation between curves for samples prepared at 88.50 MPa for three-time variables: 5 and 8-minutes produced a rapid increase in the rate of swelling within the first 10 minutes of the test, gradually levelling out thereafter and attaining a maximum displacement of ~65% and 50% respectively. Similarly, 10-minutes produced a gradual increase in swelling rate until t=8 into the experiment after which, there appears to be a linear increase to a peak at ~55%.

Aqueous NaCl Solution: 0.5 mol/L

Figure 17 shows displacement plots for mixed PWB and Quartz (at varying %) cores with different particle sizes (μm) swollen in an aqueous 0.5 mol/L NaCl solution for samples prepared at 88.50 MPa for 5, 8 or 10 minutes. This subsection will discuss these plots with increasing quartz content and decreasing grain size.

10% Quartz

Particle size: >300 μm

Mixed PWB:10% quartz cores with a grain size >300 μm that were swollen in an aqueous 0.5 mol/L NaCl solution (Figure 17) produced a somewhat rapid increase in the rate of change, for those samples prepared at 88.50 MPa for three different time variables: 5-minutes produce a curve with a gradual and steady increase on the rate of displacement to a peak value of ~90%; 8-minutes shows a curve with a rapid increase in the rate of change until t=10 when the slope gradually evens out to achieve a maximum displacement of ~125%, and 10-minutes line steadily increase displacement reaching a peak of ~100 %.

Particle size: 250-300 μm

Mixed PWB:10% quartz cores with a grain size 250-300 μm that were swollen in an aqueous 0.5 mol/L NaCl solution (Figure 17) at 88.50 MPa produced displacement curves for three different variables: 5, 8 and 10 minutes show gradually increasing rate of change for displacement, and all three change their slope when t=10 and attain peak values of close to 70%, 135% and 120% respectively.

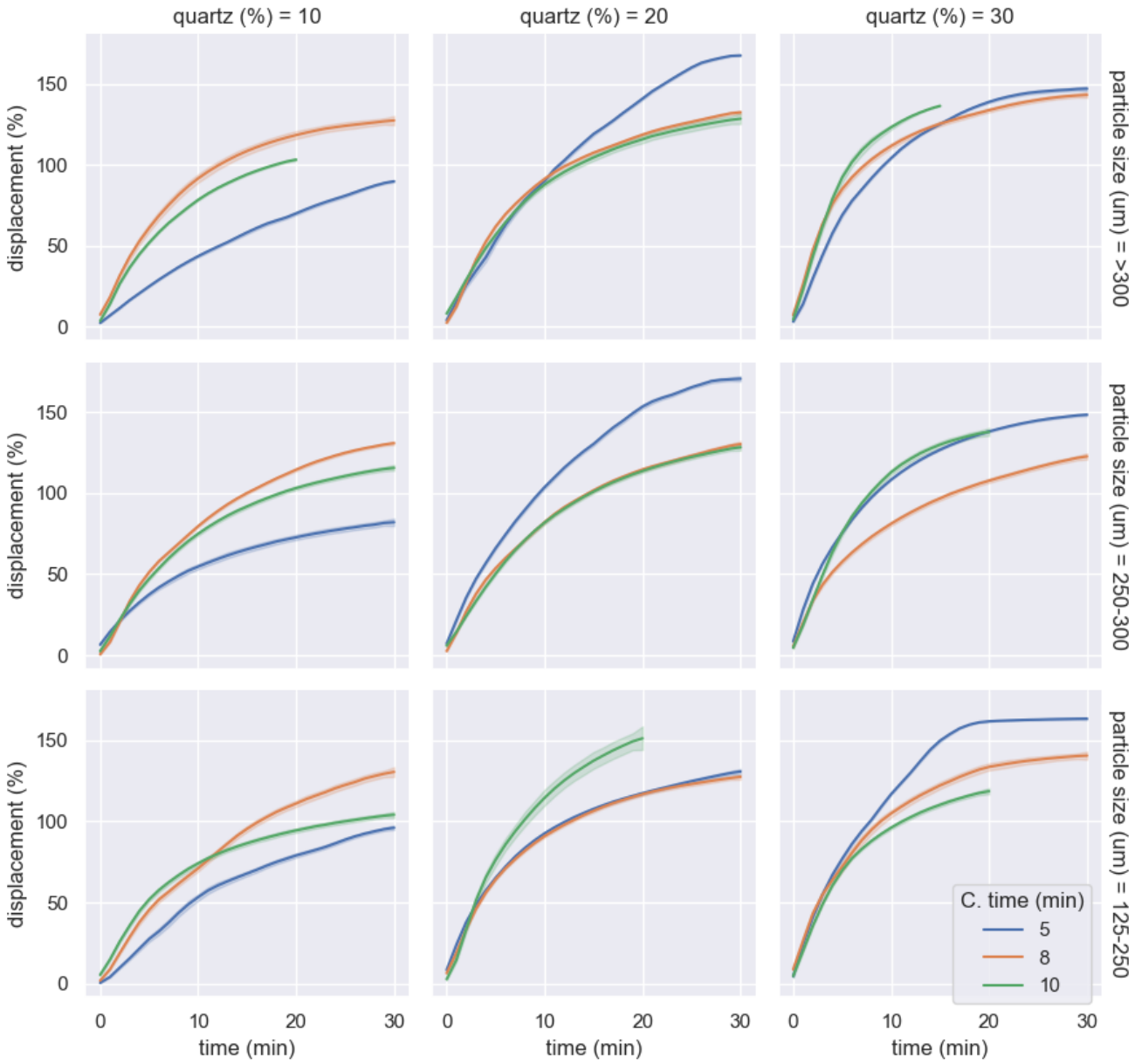

Figure 17: Mixed PWB and Quartz at 88.50 MPa in 0.5 mol/L NaCl solution - displacement data across (the average of) all sensors per minute with a shaded error region (95% confidence interval of the mean) – here all error is < 5%. The plot identifies the quartz % of the cores and their particle. Each line represents the average vertical displacement for a test where pellets were compacted for either 5 (blue), 8 (orange) or 10 (green) minutes.

Particle size: 125-250 µm

Mixed PWB:10% quartz cores with a grain size 125-250 µm that were swollen in an aqueous 0.5 mol/L NaCl solution (Figure 17), produced a generally gradual increase in the rate of change for three different time variables: 5, 8 and 10-minutes show a curve that produces a gradual increase in the rate of change until t=10 after which the slope increases for 5 and 8-minutes, and slowly flattens out for the 10-minute variable; the maximum slopes are 90%, 130% and 105% respectively.

20% Quartz

Particle size: >300 µm

Mixed PWB:20% quartz cores with a grain size >300 µm that were swollen in an aqueous 0.5 mol/L NaCl solution (Figure 17) produced some similar displacement between curves for samples prepared at 88.50 MPa with different time variables: 5, 8 and 10 minutes have curves that are almost coincident to each other, with a relatively steep gradient until just after t=10; after this point, the 5-minute curve diverges and increases the rate of change to a peak of ~170% whereas, the other two time-variables start to level out to their joint peak at ~135%.

Particle size: 250 - 300 µm

Mixed PWB:20% quartz cores with a grain size 250-300 µm that were swollen in an aqueous 0.5 mol/L NaCl solution (Figure 17) produced similar displacement curves for samples prepared at 88.50 MPa with different time variables: 5-minutes increases the rate of change steadily until t=25 when the curve plateaus and attains a maximum displacement of ~160%. Whereas, 8 and 10 minutes have curves that are coincident to each other, with a gradual increase in the rate of change with their maximum value at ~140%

Particle size: 125 - 250 µm

Mixed PWB:20% quartz cores with grain size 125- 250 µm that were swollen in an aqueous 0.5 mol/L NaCl solution (Figure 17) produced varied displacement curves for samples prepared at 88.50 MPa for different time variables: 5 and 8 minutes have curves that are coincident to

each other, with a gradual increase in the rate of change with their maximum value at ~135%. Whereas 10-minutes rapidly increases the rate of change until its peak value of ~ 150%.

30% Quartz

Particle size: >300 µm

Mixed PWB:30% quartz cores with a grain size >300 µm that were swollen in an aqueous 0.5 mol/L NaCl solution (Figure 17) produced little variation between curves for samples prepared at 88.50 MPa at different time intervals: 5, 8 and 10-minute lines produced similar curves with somewhat elevate the rate of change and achieved a maximum displacement of ~ 150%, 148% and 140% respectively.

Particle size: 250 - 300 µm

Mixed PWB:30% quartz cores with a grain size 250-300 µm that were swollen in an aqueous 0.5 mol/L NaCl solution (Figure 17) similar curves for samples prepared at 88.50 MPa at different time intervals: 5 and 10-minutes have curves that are almost on top of each other, with a somewhat rapid increase in the rate of change with their maximum value at ~ 150%; the 8-minute has a rapid increase in swelling rate until t=5 after which, the slope gradually levels out to a peak of ~125%.

Particle size: 125-250 µm

Mixed PWB:30% quartz cores with a grain size 125-250 µm that were swollen in an aqueous 0.5 mol/L NaCl solution (Figure 17) produced a wide variation between curves for samples prepared at 88.50 MPa: 5, 8 and 10-minutes have curves that have the same gradient to each other, with a rapid increase in the rate of change until they diverge at ~ 8 minutes into the test. The 5-minute curve steadily increases until t= 18, after which it plateaus with a maximum displacement of ~ 160%; whereas, the eight and 10-minute curves gradually level out until they reach their peaks at ~ 145% and 120% respectively.

Aqueous NaCl Solution: 2 mol/L

Figure 18 shows displacement plots for mixed PWB and Quartz (at varying %) cores with different particle sizes (μm) swollen in an aqueous 2 mol/L NaCl solution for samples prepared at 88.50 MPa for 5, 8 or 10 minutes. This subsection will discuss these plots with increasing quartz content and decreasing grain size.

10% Quartz

Particle size: >300 μm

Mixed PWB:10% quartz cores with a grain size >300 μm that were swollen in an aqueous 2 mol/L NaCl solution (Figure 18) produced a somewhat rapid increase in the rate of change of displacement, for those samples prepared at 88.50 MPa:

- 5 minutes shows a gradual increase in the rate of change in the first 10 minutes of the test, after which it plateaus to a peak of ~50%
- 8 and 10-minute curves show a steep and rapidly increasing rate of change, almost coincident to each other until t = 5 into the test where they diverge: 10-minutes plateaus at ~120% whereas, 8-minutes increases slightly and then plateaus at t=8 with a maximum displacement of ~ 130%.

Particle size: 250-300 μm

Mixed PWB:10% quartz cores with a grain size 250-300 μm that were swollen in an aqueous 2 mol/L NaCl solution (Figure 18) at 88.50 MPa produced similar curves at different time variables:

- Five minutes produce a curve that steadily increases the rate of change, until t=10 when it levels out at ~125%; then there is small decrease (step) at ~ t=20 and a second plateau.
- Eight and 10-minutes are coincident throughout the test and show a rapid increase in the rate of change until a plateau at ~ t = 5 minutes with a maximum displacement of ~140%.

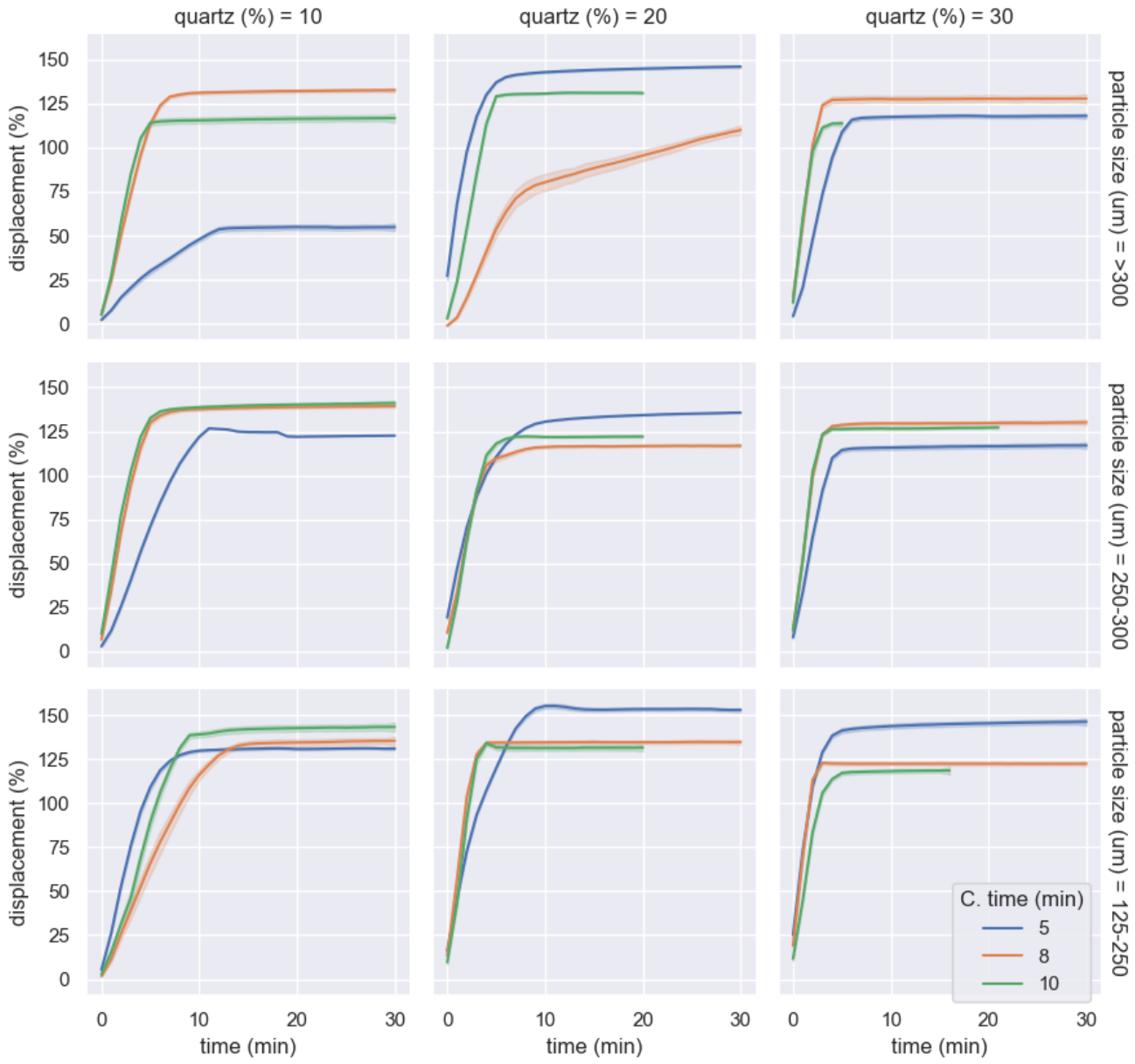

Figure 18: Mixed PWB and Quartz at 88.50 MPa in an aqueous 2 mol/L NaCl solution - displacement data across (the average of) all sensors per minute with a shaded error region (95% confidence interval of the mean) – here all error is < 2%. The plot identifies the quartz % of the cores and their particle. Each line represents the average vertical displacement for a test where pellets were compacted for either 5 (blue), 8 (orange) or 10 (green) minutes.

Particle size: 125-250 µm

Mixed PWB:10% quartz cores with a grain size 125-250 µm that were swollen in an aqueous 2 mol/L NaCl solution (Figure 18) produced three curves (5, 8 and 10 minutes) that initially have a rapid increase in the rate of swelling: 5-minutes plateaus at t=8 with a maximum displacement of ~130%; 8-minutes flattens out at t=15 with a peak at ~ 135%, and 10-minutes levels out at t=9 and has a peak displacement value of ~140%.

20% Quartz

Particle size: >300 µm

Mixed PWB:20% quartz cores with a grain size >300 µm that were swollen in an aqueous 2 mol/L NaCl solution (Figure 18) produced some variation between curves for samples prepared at 88.50 MPa: 5 and 10-minute curves show a rapid increase in the rate of change, which starts to lengthen out and eventually plateau at t=5 to its maximum displacement value of ~148% and 130% respectively. The 8-minute curve shows a somewhat rapid increase in the rate of displacement until t=8 after which the curve appears to increase swell, almost linear trend, to a maximum displacement of ~115%.

Particle size: 250 - 300 µm

Mixed PWB:20% quartz cores with a grain size 250-300 µm that were swollen in an aqueous 2 mol/L NaCl solution (Figure 18) produced similar displacement curves for samples prepared at 88.50 MPa. All three curves (5, 8 and 10 minutes) show a rapid increase in the rate of change until t=8, and they level out with maximum displacement of ~ 135%, 120% and 125% respectively

Particle size: 125 - 250 µm

Mixed PWB:20% quartz cores with grain size 125- 250 µm that were swollen in an aqueous 2 mol/L NaCl solution (Figure 18) produced some varied displacement curves for samples prepared at 88.50 MPa: All three curves (5, 8 and 10 minutes) initially have a steep linear trend coincident to each other: The 5-minute curve diverges from the other two plots at t=2 and

increases until it plateaus at t=10 with a peak displacement of ~155%; whereas, the eight and 10-minute lines remain together and plateau at t=5 with a maximum swell at ~130%.

30% Quartz

Particle size: >300 µm

Mixed PWB: 30% quartz cores with a grain size >300 µm that were swollen in an aqueous 2 mol/L NaCl solution (Figure 18) produced some variation between curves prepared at 88.50 MPa for the time variables: 5, 8 and 10 minutes. The curves produced a very rapid increase in the rate of change, and all three plateaued between 2-5 minutes of the test to have a maximum displacement value of ~ 120%, 125% and 118% respectively.

Particle size: 250 - 300 µm

Mixed PWB:30% quartz cores with a grain size 250-300 µm that were swollen in an aqueous 2 mol/L NaCl solution (Figure 18) produced little variation between curves for samples prepared at 88.50 MPa for three-time variables: 5, 8 and 10-minute curves produced a very rapid increase in the rate of change. Five minutes had a slightly shallower gradient than the other two time-variables, which plateaued at 5 minutes with a peak of ~118%; whereas, eight and 10-minutes produced curves coincident with each other, both flattening out from 2.5 minutes and attaining a peak of ~130%.

Particle size: 125-250 µm

Mixed PWB:30% quartz cores with a grain size 125-250 µm that were swollen in deionised water (Figure 18) produced a small variation between curves for samples prepared at 88.50 MPa for three-time variables: 5, 8 and 10-minute curves show a rapid increase in the rate of change for displacement until they reach their final (and maximum) swell and plateau at ~ 150%, 125% and 120% respectively.

Statistical Analysis

ANOVA

The average maximum swell for all variables was calculated, and their associated p-values were produced using ANOVA analysis of variance. The p-values indicate how likely means of the variable-levels deviate from each other.

The variables that were found to be significant ($p < 0.05$) were then plotted graphically to visually assess their effect (Figure 19, Discussion): Compression time ($p < 0.001$), pressure ($p = 0.37$), quartz ($p < 0.05$**),** particle size ($p < 0.464$) and concentration ($p < 0.001$)**.**

Linear Regression

The linear regression for the rate of change showed a coefficient (the change in rate (%) per minute) with an associate p-value to indicate the significance of:

Changing the concentration of quartz from Bentonite-only (0% quartz) to:

- 10% Quartz produces a non-significant effect ($p = 0.63$) with a coefficient of 1.18 (±2.45 standard error) displacement % per minute
- 20% produces a very significant effect ($p < 0.01$) with a coefficient of 7.91 (±2.45 standard error) displacement % per minute
- 30% produces an extremely significant effect ($p < 0.001$) with a coefficient of 11.67 (±2.47 standard error) displacement % per minute

Increasing the compression time that artificial cores were pressed for from 5 minutes to:

- 8 minutes produced a non-significant effect ($p = 0.326$) with a coefficient of -2.62 (±2.66 standard error) displacement % per minute;
- 10 minutes produced a non-significant effect ($p = 0.12$) with a coefficient of -4.28 (±2.75 standard error) displacement % per minute

Changing the fluid that the cores were swollen in from deionised water (0 M) to an aqueous NaCl concentration of:

- 0.5 mol/L produced an extremely significant effect ($p < 0.001$) with a coefficient of 52.92 (±2.7 standard error) displacement % per minute
- 2 mol/L produced an extremely significant effect ($p < 0.001$) with a coefficient of 82.36 (±2.85 standard error) displacement % per minute

Changing the particle size from bentonite-only (around 8 μm) to:

- 125-250 μm produced a highly significant effect ($p < 0.01$) with a coefficient of 7.09 (±2.45 standard error) displacement % per minute
- >250-300 μm produced a very significant effect ($p < 0.01$) with a coefficient of 6.55 (±2.45 standard error) displacement % per minute
- >300 μm produced a very significant effect ($p < 0.01$) with a coefficient of 7.12 (±2.46 standard error) displacement % per minute

Changes within the particle size range 125 μm to >300 μm do not appear to have a significant effect but are very significant relative to bentonite-only.

Discussion

This study provides high-resolution data from linear displacement measurements. These swelling experiments involve monitoring the one-dimensional displacement with the time of an initially dry artificial core as it imbibes liquid from a supply at its base.

In this chapter we will endeavour to elucidate the results from this study and ascertain potential implications.

Vertical Displacement of Bentonite Cores

When the composition of the artificial core is 100% pure Wyoming Bentonite, then the samples are homogeneous and; compaction time, pressure and swelling solution concentration (salinity) are the changing variables considered here.

Short-term swelling tests (30 minutes) of bentonite-only cores produced displacement curves that usually had rapid initial swelling within the first 10 minutes of the experiment, after which the rate of change for displacement would either gradually level out or plateau (i.e. no more swelling occurred). This rapid increase in the primary stages, <10 minutes into many of the swelling tests, is likely due to macroscopic swelling from accessible void space in the artificial core with overall reduced internal swelling pressure (van Oort et al., 2003 & 2016).

The gradual flattening of the swelling curves in the secondary stage (>10 minutes) is likely resultant because of a decrease in void space, which in turn increases the pore pressure in the remaining pores and increases the swelling pressure; crystalline swelling expands the interlayers within the bentonite aggregates (Anderson et al., 2010).

For the same swelling solution concentration(s), displacement curves appear to produce similar maximum swell and rate of change for the two compaction pressures. Similarly, compaction time (i.e. the time at which the pressure that core has been kept) does not differ significantly between pressures. However, individually for the same plots, compaction time produces a difference of ~ 10% between each time. For the same concentration but at different pressures, the compaction times produce a similar trend. These trends indicate that the differences seen in displacement are due to changes in the structure (e.g. fissility, cleavage, microfractures) and the resulting physio-chemical forces acting on the fabric (van Oort et al., 2003 & 2016; Wilson & Wilson, 2014).

However, as the concentration of NaCl increases the maximum swell increases along with a rapid rate of change in the primary stages of the test, which indicates that concentration (i.e. salinity) has a significant impact upon increasing swelling rate. Na-montmorillonite has a

high CEC and combined with Na^+ in the NaCl solution, gives rise to higher osmotic pressures (van Oort et al., 2003; Anderson et al., 2010); which might explain the significant volume increase with an increase in concentration (Figure 19).

Vertical Displacement of Mixed Bentonite-Quartz Cores

Here artificial cores are comprised of Pure Wyoming Bentonite (PWB) with a quartz content of 10%, 20% and 30% quartz. Where quartz was introduced into the 'shale' preparation, size fractions were varied: 125-250 μm, >250-300 μm and >300 μm. These cores were prepared under different conditions by varying: The pressure (44.25 and 88.50 MPa) and time (5, 8 and 10 minutes) that they were compacted. Cores were partially submerged in either deionised water (labelled as 0 M) or an aqueous solution (sodium chloride at either 0.5 or 2 mol/L).

Short-term swelling tests (30 minutes) for mixed PWB: Quartz cores showed that for the same quartz content (%), regardless of pressure (44.25 and 88.50 MPa), at the same salinity, displacement curves produced similar trends with minimal variation despite increasing particle sizes; comparative tests (same variables) with different times of compaction produced the most noticeable variation between different variables.

However, if the concentration of the swelling solution increases, quartz content and particle size appear to have a much higher effect upon vertical displacement. The displacement is likely due to the broader distribution of pores sizes introduced to the samples as quartz content and particle size increases, swelling is rapid and variation between tests increases due to inhomogeneity.

Increased pore spaces (porosity) result in decreased resistance to swelling. Here too, the time at which the cores are compacted for (pressure does not seem to make much impact upon increasing or decreasing swelling) has a much more significant effect upon a reduction in permeability and resulting capillary pressures. As bentonite content reduces, the capacity at which the clay platelets swell and 'seal' (reduce permeability) the core reduces, thereby increasing the swelling from the primary (<10 minutes into the test) into the second phase as a result of macroscopic swelling having the opportunity to continue for longer. This reduction in overall permeability increased porosity and increasingly less bentonite component results in sloughing (slumping/collapse) of the samples as salinity concentration increases leading to the more substantial variability and stepped (sometimes decreasing) changes in rate.

According to Wilson & Wilson (2014), an overlap of the diffuse double layer (DDL) with the exposed clay minerals on disparate sides of existing (within the clay), and secondary

mesopores, pores would induce electrostatic repulsion. This would result in increased pore and swelling pressure in the artificial shale (cores).

Variables

Figure 19 is a plot of the average maximum swell across all the data (bentonite-only and PWB: quartz) with three specific and significant (identified using ANOVA statistical analysis) variables:

- Compression time (Fig.19a) indicates that the maximum swelling of an artificial core is affected by how long it has been pressed for during preparation, regardless of the pressure (44.25 or 88.50 MPa) applied to it
- Concentration (Fig.19b) increases from deionised water (0 mol/L) to either 0.5 or 2 mol/L NaCl solution. It illustrates how significant (saline) concentration is upon increasing vertical displacement. Deionised water produces the least swell at ~ 70%; 0.5 mol/L NaCl has peak swell at ~135%, and 2 mol/L NaCl maximum swell at ~130%
- Quartz content (Fig.19c) from Bentonite-only (0 %) has a maximum swell of 106%; 10% Quartz increases swell up to 108%; 20% Quartz jumps to a peak of 118%, and increasing quartz content to 30% reduces maximum swell to 110%

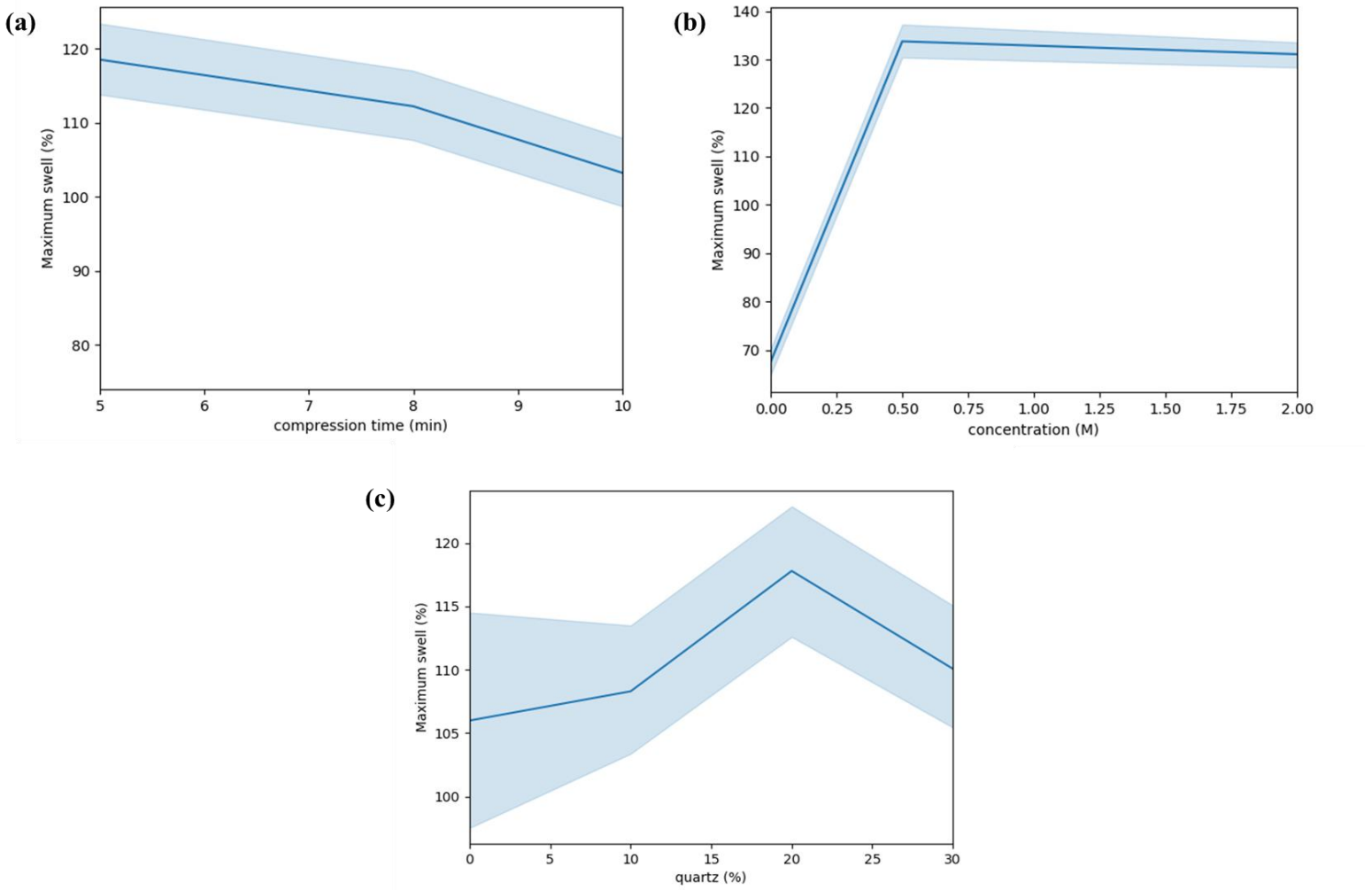

Figure 19 – Plots of Maximum Vertical Displacement (swell) vs. Significant Variables for both 44.25 and 88.50 MPa: **(a)** Maximum Swell vs. Compression Time, and their associated error shading (95% confidence interval of the mean); **(b)** Maximum Swell vs. Aqueous NaCl Solution Concentration, and **(c)** Maximum Swell vs. Quartz Content.

Shale Mineralogy and Microstructure

Sample preparation introduced: Texture, which is the relative proportions of content and particle size which make up the 'shale'; a structure which is the arrangement of features and the components in the (artificial) rock (Wilson and Wilson, 2014); and finally, the fabric which is the spatial relationship of clay and other constituent particles which creates pores and voids in the core.

Figure 20 is a schematic representation of how texture and salinity increase the swelling capabilities of samples in this study. Variations in texture result in a change from vertical swelling (PWB) only, to both vertical and lateral displacement. For specific samples with >10% quartz at a concentration between 0.5 and 2 mol/L NaCl, there appears to be a threshold above which a transition from anisotropic to isotropic swelling may be seen. This transition threshold is influenced by increasing particle size; due to a decrease in the space availability within macropores for the bentonite to swell (Saba et al., 2014; Wilson & Wilson, 2014).

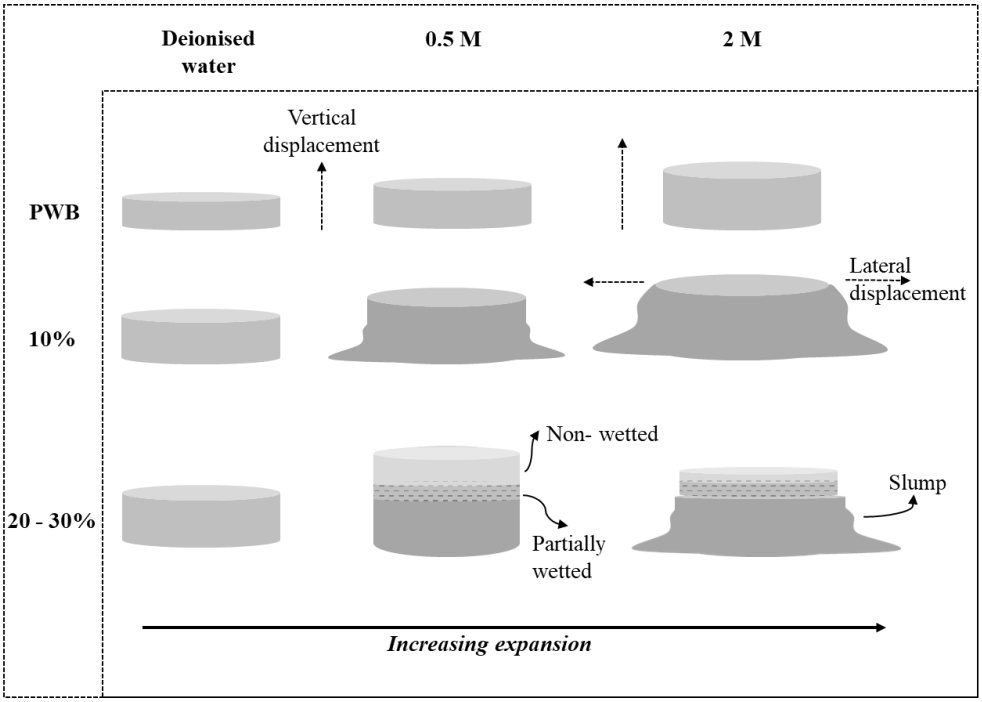

Figure 20 – Schematic diagram of the physical swelling properties for individual artificial cores (outside of the holder): Quartz content (%) plotted against Water-NaCl solutions (deionised water, 0.5 and 2 mol/L (M)) , where PWB is bentonite-only, and the solution that the test used. The dashed section indicates a wet-dry boundary.

The different structures produced in this study (homogenous vs heterogeneous) can potentially help better understand the implication that structure has an effect on shale and its instability in the wellbore. Composite cores are more representative of natural shale, which are heterogeneous materials (Wilson and Wilson, 2014), despite being a simplified system containing only two components (bentonite-quartz). Increasing heterogeneity introduced microfractures within the system, which formed under compaction/pressure. These microfractures introduce pathways for the fluid.

Time and pressure were varied to simulate a simplified diagenetic process. The data implies that increasing burial depth (i.e. pressure increase) does not have as much impact upon swelling and instability as previously thought. Instead, it is the age of the sediment (i.e. compaction time) that has, potentially, the most significant impact upon the structure of the rock.

Although the fabric was not explicitly analysed, an inference can be made about the orientation of the clay minerals. Most shales are assumed to be well orientated, but many have an indiscriminate layering of platy minerals.

Here, Bentonite-only and PWB:10% Quartz samples have well-orientated fabric. However, samples with > 20% quartz have a higher porosity due to less fabric orientation; this may explain for why the samples either dispersed or disintegrated when swollen in aqueous solution (> 0.5 mol/L).

Implications from Research

The data in this study can make inferences about shale and what may cause their instability. The preparation of samples and swelling data from this report may be used to make inferences about how the mineralogy and microstructure in shale can influence, and potentially cause, instability in a wellbore. The research provides useful insights for sample preparation in a laboratory, wellbore stability, radioactive waste repositories and soil mechanics (for civil engineering).

This study attempted to simulate a simplified diagenetic process, and the data implies that increasing burial depth (i.e. pressure increase) has a less significant effect upon swelling and instability than previously thought. Instead, the age of the sediment (i.e. compaction time) appears to have the most significant impact upon the structure of the rock, and thereby, the swelling.

Interestingly, as the samples move from clay – shale - sandy mudstone – wacke (<50% clay matrix), the rate of volume change in the sample increases above that of the Pure Wyoming Bentonite and the PWB:10, which are representative of a sloughing-shale. The overall stability of the sample is significantly reduced (Fig.20). During drilling, therefore, it would be useful to not only to consider an enhanced method whilst running laboratory testing on cuttings, but also the geology of the rock; it is of significance to its behaviour both in situ, but when testing (even when recompacted). The bedding plane orientation in shale is critical; it is at an angle; the increased surface area exposed to the drill may result in an increased swell-response. However, this will depend upon on the inclination angle, mineralogy and diagenetic history.

The reduction in overall permeability and increased results in sloughing (slumping/collapse) of the samples as salinity concentration increases, leading to the more substantial variability and stepped (sometimes decreasing) rate changes. These stepped changes in rate are an interesting effect seen only with 0.5 and 2 mol/L and are highly reproducible. Classical theory predicts that inverse overall swelling relative to ionic strength (i.e. equilibrium conditions) should be seen. However, there is nothing to say of its kinetics – this would require further investigation (discussed in the Future Work section). It is therefore unusual that there appears to be a threshold above which a transition from anisotropic to isotropic swellings occurs.

Similarly, samples with higher quartz content >10% (including 30% tests run, see Methods) appear to experience sticking or a suction effect, similar to ‘bit balling’ seen in the petroleum industry, when in contact with a metallic, smooth surface, especially under pressure. Whilst more tests would be required to investigate this effect, a rougher surface or colloidal coating with texture should be used on a drill bit to reduce suction and would likely prevent this during drilling.

Some formations with water-sensitive clays do not always exhibit swelling behaviour, and it can be challenging to predict the response of these rocks to aqueous fluids downhole. Dispersing capabilities, cementation, bedding orientation (i.e. diagenetic history) and pore water chemistry are all significant. Preparation of rock cutting samples is vital to the outcome of laboratory (swelling) research confirming field analysis. The preparation of pellets for swelling-interaction studies require consistency and representative pressure/time to reproduce diagenetic effects, which alter the behaviour of rocks during drilling. The data suggests that we may not always see failure within formations, despite having the mineralogy to support swelling-theory.

Conclusion

The swelling response of shale was studied to understand swelling-mechanisms, and potential causes, that lead to shale instability. The relationship between mineralogical composition, compaction pressure and formation age were investigated and related to shale-fluid interaction mechanisms within a wellbore region.

Some formations containing water-sensitive clays do not always exhibit swelling behaviour, and it can be challenging to predict the response of these rocks to aqueous fluids downhole. Compacted bentonite is typically used in experiments and models to predict the effect that swelling inhibitors have upon shales (Mathias et al., 2017).

This study has concluded that changing variables during sample preparation has a significant impact on real displacement data; some of which may account for some reproducibility problems encountered in literature, especially when compared to field analysis.

The results indicate that:

- The time that a sample pressed for is more significant than the pressure (44.25 or 88.50 MPa) applied to it**,**
- Changing the fluid that the cores were swollen in from (deionised) water to an aqueous (NaCl) concentration with increasing molarity increased the rate of displacement**,**
- Increasing the quartz content (%) had a very significant effect upon the swelling rate
- Changes within the particle size range 125 to >300 μm do not appear to have a significant effect overall but are very significant relative to bentonite-only samples
- In samples with >10% quartz and swollen in a NaCl solution 0.5-2 mol/L, there appears to be a threshold above which a transition from anisotropic to isotropic swelling occurs**.**

Future Work

If this project were to be pursued for further research, laboratory and non-destructive tests should be used to consolidate and provide further information on shale microstructure and fabric with relation to the effect of different variables upon swelling mechanisms.

Re-run non-linear displacement meter (NLDM) tests of samples that produced delayed swelling using larger holders to allow for horizontal swelling. These larger holders have been designed by Tara Love, Prof. Chris Greenwell and The Physics Department workshop (Durham University), in preparation for these upcoming experiments. These larger sample holders will allow horizontal displacement to occur if it does, and interpretation can be made as to whether there is a shift between anisotropic to isotropic swelling.

X-ray Diffraction (XRD) should be used to aid with interpretation for the anisotropic swell to ascertain D-spacing and if the orientation of clay platelets has changed during the preparation of samples. *In situ* swelling in XRD, using the wet-cell XRD method provided by Erdogan (2014) should be incorporated to provide measurements on the kinetics of clay swelling and the role of interlayer expansion during displacement measurements.

Furthermore, imaging using Scanning Electron Microscopy (SEM) and X-ray Computed Tomography (XRCT) of samples to ascertain internal and external fabric and microstructure should be incorporated. These imaging techniques were attempted during this project briefly. However, due to time constraints, this method was put on hold. There is a requirement to image multiple samples beforehand to improve the scanning technique and get the voxel size down to between 2 - 4 microns resolution, as many particles are below normal thresholds without this improvement.

References

Albukhari, TAREQ M., GHAITH K. Beshish, MOFTAH M. Abouzbeda, and A. B. D. A. S. A. L. A. M. Madi. "Geomechanical Wellbore Stability Analysis for the Reservoir Section in JNC186 Oil Field." In 1st International Conference on Advances in Rock Mechanics-TuniRock 2018. International Society for Rock Mechanics and Rock Engineering, 2018.

Anderson, R.L. et al., 2010. Clay swelling - A challenge in the oilfield. Earth-Science Reviews, 98(3-4), pp.201–216

Caenn, R., Darley, H.C. and Gray, G.R., 2011. Composition and properties of drilling and completion fluids. Gulf professional publishing.

Chan, A.W., Yadav, S. and Mikulencak, D.R., 2019. From Wellbore Instability and Grain Mixing to Injectivity Reduction. Rock Mechanics and Rock Engineering, pp.1-10.

Cheatham Jr, J.B., 1984. Wellbore stability. Journal of petroleum technology, 36(06), pp.889-896.

Cheatham, C.A. and Nahm, J.J., 1990, January. Bit balling in water-reactive shale during full-scale drilling rate tests. In SPE/IADC Drilling Conference. Society of Petroleum Engineers.

Chen, J., Lan, H., Macciotta, R., Wu, Y., Li, Q. and Zhao, X., 2018. Anisotropy rather than transverse isotropy in Longmaxi shale and the potential role of tectonic stress. Engineering Geology, 247, pp.38-47.

Cho, G.C., Dodds, J. and Santamarina, J.C., 2004. Particle Shape Effects on Packing Density. Stiffness and Strength of Natural and Crushed Sands-Internal Report, Georgia Institute of Technology, 33pp.

Civan, F., 2015. Reservoir formation damage. Gulf Professional Publishing.

Cook, J., Growcock, F., Guo, Q., Hodder, M. and van Oort, E., 2011. Stabilizing the wellbore to prevent lost circulation. Oilfield Review, 23(4), pp.26-35.

Du, J., Hu, L., Meegoda, J.N. and Zhang, G., 2018. Shale softening: Observations, phenomenological behavior, and mechanisms. Applied Clay Science, 161, pp.290-300.

Erdogan, A., 2016. Interpretation of clay swelling via non-contact linear displacement meter (NC-LDM) (Doctoral dissertation, Durham University).

Ezzat, A.M., 1990, January. Completion fluids design criteria and current technology weaknesses. In SPE Formation Damage Control Symposium. Society of Petroleum Engineers.

Fattah, M.Y. and Al-Lami, A.H., 2016. Behavior and characteristics of compacted expansive unsaturated bentonite-sand mixture. Journal of Rock Mechanics and Geotechnical Engineering, 8(5), pp.629-639.

Fink, J., 2015. Water-base chemicals and technology for drilling, completion, and workover fluids. Gulf Professional Publishing.

Friedheim, J., Guo, Q., Young, S. and Gomez, S., 2011, January. Testing and evaluation techniques for drilling fluids-shale interaction and shale stability. In 45th US Rock Mechanics/Geomechanics Symposium. American Rock Mechanics Association.

Gholami, R., Elochukwu, H., Fakhari, N. and Sarmadivaleh, M., 2018. A review on borehole instability in active shale formations: interactions, mechanisms and inhibitors. Earth-science reviews, 177, pp.2-13.

Grim, R. E. 1953. Clay mineralogy. Soil Science, 76, 317.

HALE, A. H., MODY, F. K. & SALISBURY, D. P. 1993. The Influence of Chemical Potential on Wellbore Stability. SPE Drilling & Completion

Hawkes, C.D., McLellan, P.J., Maurer, W.C. and Ruan, C.G., 2000. Wellbore instability in shales: a review of fundamental principles and GRI-funded research. GRI Final Report, 99(0025.3), pp.A2-A4.

Howie, R.A., Zussman, J. and Deer, W., 1992. An introduction to rock-forming minerals. Pearson Education Limited.

Huang, Z., Xu, Z., Quan, Y., Jia, H., Li, J., Li, Q., Chen, Z. and Pu, K., 2018, July. A review of treatment methods for oil-base drill cuttings. In IOP Conference Series: Earth and Environmental Science (Vol. 170, No. 2, p. 022074). IOP Publishing.

Industrimigas. 2014. IndustriMigas | #1 Oil and Gas Blog. [Online]. [6 May 2019]. Available from: http://www.industrimigas.com/2013/06/drilling-and-casing-wellbore.html

Jones E, Oliphant E, Peterson P, et al. SciPy: Open Source Scientific Tools for Python, 2001-, http://www.scipy.org/ [Online; accessed 2019-10-13].

Komine, H. and Ogata, N., 1994. Experimental study on swelling characteristics of compacted bentonite. Canadian geotechnical journal, 31(4), pp.478-490.

Mathias, S.A., Greenwell, H.C., Withers, C., Erdogan, A.R., McElwaine, J.N. and MacMinn, C., 2017. Analytical solution for clay plug swelling experiments. Applied Clay Science, 149, pp.75-78.

MODY, F. K. & HALE, A. K. 1993. Borehole stability in shales. SPE Drilling & Completion.

Mollins, L.H., Stewart, D.I. and Cousens, T.W., 1996. Predicting the properties of bentonite-sand mixtures. Clay Minerals, 31(2), pp.243-252.

Nichols, G., 2009. Sedimentology and stratigraphy. John Wiley & Sons.

O'Brien, D.E. and Chenevert, M.E., 1973. Stabilizing sensitive shales with inhibited, potassium-base drilling fluids. Journal of Petroleum Technology, 25(09), pp.1-089.

Ouadfeul, S.A. and Aliouane, L., 2015, September. Wellbore Stability in Shale Gas Reservoirs, A Case Study fromThe Barnett Shale. In SPE North Africa Technical Conference and Exhibition. Society of Petroleum Engineers.

Patel, A. and Gomez, S., 2013, April. Shale inhibition: what works?. In 2013 SPE International Symposium on Oilfield Chemistry.

Saba, S., Barnichon, J.D., Cui, Y.J., Tang, A.M. and Delage, P., 2014. Microstructure and anisotropic swelling behaviour of compacted bentonite/sand mixture. Journal of Rock Mechanics and Geotechnical Engineering, 6(2), pp.126-132.

Santarelli, F.J. and Carminati, S., 1995, January. Do shales swell? A critical review of available evidence. In SPE/IADC Drilling Conference. Society of Petroleum Engineers.

Schanz, T., Rawat, A. and Baille, W., 2016. Discussion of “Evaluation of the swelling characteristics of bentonite-sand mixtures”. Engineering Geology, (209), pp.209-210.

SCHIEBER, J., 1989. Facies and origin of shales from the mid-Proterozoic Newland Formation, Belt Basin, Montana, USA. Sedimentology, 36(2), pp.203-219.

Schneider, J., Flemings, P.B., Day-Stirrat, R.J. and Germaine, J.T., 2011. Insights into pore-scale controls on mudstone permeability through resedimentation experiments. Geology, 39(11), pp.1011-1014.

Scikit-learn: Machine Learning in Python, Pedregosa et al., JMLR 12, pp. 2825-2830, 2011

Seabold, S., & Perktold, J. (2010, June). Statsmodels: Econometric and statistical modeling with python. In Proceedings of the 9th Python in Science Conference (Vol. 57, p. 61). Scipy.

Shirazi, S.M., Wiwat, S., Kazama, H., Kuwano, J. and Shaaban, M.G., 2011. Salinity effect on swelling characteristics of compacted bentonite. Environment Protection Engineering, 37(2), pp.65-74.

Smil, V., 2016. Energy transitions: global and national perspectives. ABC-CLIO.

Stahle, L., & Wold, S. (1989). Analysis of variance (ANOVA). Chemometrics and intelligent laboratory systems, 6(4), 259-272.

Steiger, R.P. and Leung, P.K., 1992. Quantitative determination of the mechanical properties of shales. SPE drilling engineering, 7(03), pp.181-185.

Stephens, M., Gomez-Nava, S. and Churan, M., 2009, March. Laboratory methods to assess shale reactivity with drilling fluids. In AADE National Technical Conference, New Orleans.

Sun, D.A., Cui, H. and Sun, W., 2009. Swelling of compacted sand–bentonite mixtures. Applied Clay Science, 43(3), pp.485-492.

Sun, W.J., Wei, Z.F., Sun, D.A., Liu, S.Q., Fatahi, B. and Wang, X.Q., 2015. Evaluation of the swelling characteristics of bentonite–sand mixtures. Engineering Geology, 199, pp.1-11.

Tang, Q., Katsumi, T., Inui, T. and Li, Z., 2014. Membrane behavior of bentonite-amended compacted clay. Soils and Foundations, 54(3), pp.329-344.

Tucker, M.E. ed., 2009. Sedimentary petrology: an introduction to the origin of sedimentary rocks. John Wiley & Sons.

van Oort, E., 2003. On the physical and chemical stability of shales. Journal of Petroleum Science and Engineering, 38(3-4), pp.213-235.

van Oort, E., Hoxha, B.B., Hale, A., Aldin, M. and Patterson, R., 2016, April. How to test fluids for shale compatibility. In Proceedings of the AADE Fluids Technical Conference and Exhibition, Houston, TX, USA (pp. 12-13).

Wang, H., Soliman, M.Y., Towler, B.F. and Shan, Z., 2009, January. Strengthening a wellbore with multiple fractures: further investigation of factors for strengthening a wellbore. In 43rd US Rock Mechanics Symposium & 4th US-Canada Rock Mechanics Symposium. American Rock Mechanics Association.

Wang, Q., Tang, A.M., Cui, Y.J., Delage, P. and Gatmiri, B., 2012. Experimental study on the swelling behaviour of bentonite/claystone mixture. Engineering Geology, 124, pp.59-66.

Warr, L. and Berger, J., 2007. Hydration of bentonite in natural waters: application of “confined volume” wet-cell X-ray diffractometry. Physics and Chemistry of the Earth, Parts A/B/C, 32(1), pp.247-258.

Whitfill, D.L. and Nance, W., 2008. DEA 13-Investigation of Lost Circulation with Oil-base Muds (1985-1988).

Wilson, M.J., Wilson, L. and Shaw, H., 2014. Clay mineralogy and shale instability: an alternative conceptual analysis. Clay Minerals, 49(2), pp.127-145.

Zeynali, M. E. (2012). "Mechanical and physico-chemical aspects of wellbore stability during drilling operations." Journal of Petroleum Science and Engineering 82-83: 120-124.

Zheng, Y., Zaoui, A. and Shahrour, I., 2011. A theoretical study of swelling and shrinking of hydrated Wyoming montmorillonite. Applied Clay Science, 51(1), pp.177-181.